REDUCTION OF TRANSMITTER INTERMODULATION PRODUCT SIGNALS IN AIR FORCE COMMUNICATIONS SYSTEMS

N. Worontzoff, et al

AIL

Prepared for:

Rome Air Development Center

December 1972

RADC-TR-72-312
Final Technical Report
December 1972

REDUCTION OF TRANSMITTER INTERMODULATION PRODUCT SIGNALS IN AIR FORCE COMMUNICATIONS SYSTEMS

AIL Division of Cutler Hammer, Incorporated

Details of illustrations in this document may be better studied on microfiche

Rome Air Development Center
Air Force Systems Command
Griffiss Air Force Base, New York

UNCLASSIFIED

Security Classification

DOCUMENT CONTROL DATA - R & D

(Security classification of title, body of abstract and indexing annotation must be entered when the overall report is classified)

1. ORIGINATING ACTIVITY (Corporate author)	2a. REPORT SECURITY CLASSIFICATION
AIL Division of Cutler Hammer, Incorporated Deer Park, New York 11729	UNCLASSIFIED
	2b. GROUP N/A

3. REPORT TITLE

REDUCTION OF TRANSMITTER INTERMODULATION PRODUCT SIGNALS IN AIR FORCE COMMUNICATIONS SYSTEMS

4. DESCRIPTIVE NOTES *(Type of report and inclusive dates)*

Final Report March 1971 through March 1972

5. AUTHOR(S) *(First name, middle initial, last name)*

N. Worontzoff
H. Levy
Y. DeGruyl

6. REPORT DATE	7a. TOTAL NO. OF PAGES	7b. NO. OF REFS
December 1972	~~58~~ 64	7

8a. CONTRACT OR GRANT NO.	9a. ORIGINATOR'S REPORT NUMBER(S)
F30602-71-C-0222	5365-1
b. PROJECT NO Job Order No. 45400350	
c.	9b. OTHER REPORT NO(S) *(Any other numbers that may be assigned this report)*
d.	RADC-TR-72-312

10. DISTRIBUTION STATEMENT

Approved for public release; distribution unlimited.

11. SUPPLEMENTARY NOTES	12. SPONSORING MILITARY ACTIVITY
None Details of illustrations in this document may be better studied on microfiche	Rome Air Development Center (RBCI) Griffiss Air Force Base, New York 13441

13. ABSTRACT

This report describes the results of a program investigating means of reducing the intermodulation products generated in collocated 100-watt transmitters operating in the 225 to 400 MHz frequency range. The IM reduction technique considered a cascade of four tunable isolators and a standard tunable filter to achieve a net antenna-to-transmitter isolation of 80 dB.

The major accomplishment on this program was the development of a tunable, compact, lumped-parameter UHF isolator having a power handling level in excess of 100 watts with a typical forward loss of 0.5 dB, and a 20-dB isolation bandwidth of 4.3 to 7.6 percent. Although the cascade of these isolators and a tunable filter will provide the required transmitter intermodulation protection, the IM level generated by the first isolator in the chain was -40 dBm for the maximum power conditions of +50 dBm main signal and +20 dBm interfering signal.

Replacement of the first isolator with a standard distributed type isolator would reduce the IM level to -60 dBm, still short of the design goal. Considerable effort was expended in an attempt to fully understand the mechanism for IM generation and lower the level to the -70 to -80 dBm objective. Although a greater understanding in ferrite isolation has been gained, further reduction of the IM level was not realized.

DD FORM 1 NOV 65 1473

UNCLASSIFIED

Security Classification

UNCLASSIFIED

Security Classification

14 KEY WORDS	LINK A		LINK B		LINK C	
	ROLE	WT	ROLE	WT	ROLE	WT
Intermodulation Product Reduction Tunable UHF Isolator						

ib

UNCLASSIFIED

Security Classification

SAC--Griffiss AFB NY

REDUCTION OF TRANSMITTER INTERMODULATION PRODUCT SIGNALS IN AIR FORCE COMMUNICATIONS SYSTEMS

N. Worontzoff
H. Levy
Y. DeGruyl

AIL Division of Cutler Hammer, Incorporated

ic

FOREWORD

This is the final report on contract F30602-71-C-0222, Job Order Number 45400350, by AIL division of Cutler Hammer, Incorporated, Deer Park, New York, for Rome Air Development Center, Griffiss Air Force Base, New York. The management and technical supervision of this program was initially under the cognizance of Captain Gary Seasholtz (RBCI) and later transferred to Mr. Frederick Moore (RBCI). AIL personnel who contributed to this report are Engineers H. Levy and N. Worontzoff; Department Consultant Y. DeGruyl and Division Consultant J. Taub; Department Head R. Sleven; and Technician S. Davis.

The work described in this report was performed between March 1971 and March 1972. The report was numbered by AIL 5365-1.

This report was reviewed by the RADC Information Office (OI) and is releasable to the National Technical Information Service (NTIS).

This technical report has been reviewed and is approved.

Approved:
JOHN E. ERICKSON, CAPT, USAF
Interf Anal & Control Section
Compatibility Branch

Approved:
JOSEPH J. NARESKY
Chief, Reliability & Compatibility Division

FOR THE COMMANDER:

FRED I. DIAMOND
Chief, Plans Office

ABSTRACT

This report describes the results of a program investigating means of reducing the intermodulation products generated in collocated 100-watt transmitters operating in the 225 to 400 MHz frequency range. The IM reduction technique considered a cascade of four tunable isolators and a standard tunable filter to achieve a net antenna-to-transmitter isolation of 80 dB.

The major accomplishment on this program was the development of a tunable, compact, lumped-parameter UHF isolator having a power handling level in excess of 100 watts with a typical forward loss of 0.5 dB, and a 20-dB isolation bandwidth of 4.3 to 7.6 percent. Although the cascade of these isolators and a tunable filter will provide the required transmitter intermodulation protection, the IM level generated by the first isolator in the chain was -40 dBm for the maximum power conditions of +50 dBm main signal and +20 dBm interfering signal.

Replacement of the first isolator with a standard distributed type isolator would reduce the IM level to -60 dBm, still short of the design goal. Considerable effort was expended in an attempt to fully understand the mechanism for IM generation and lower the level to the -70 to -80 dBm objective. Although a greater understanding of IM generation in ferrite isolation has been gained, further reduction of the IM level has not been realized. However, all of the techniques formulated for accomplishing the IM reduction have not yet been fully implemented and the possibility of -80 dBm still exists.

REDUCTION OF TRANSMITTER INTERMODULATION PRODUCT SIGNALS IN AIR FORCE COMMUNICATIONS SYSTEMS

1. The overall objective of this contractual effort was to develop ways to reduce intermodulation products due to collocated transmitters operating in the 225 to 400 MHz frequency range. The system to be developed must be suitable for signals with essentially zero frequency separation as well as for signals with large frequency separations.

2. The specific objective was to develop a tunable, compact, lumped - parameter UHF isolator with a power handling capability of 100 watts, an isolation of 20 dB, and an insertion loss of no greater than 0.5 dB. The design goal was to make the intermodulation product, generated by the circulator, less than -70 dBm when a signal of +50 dBm is fed forward through the circulator and another signal of +20 dBm is fed into the circulator from the reverse direction.

3. The circulator developed under this contract successfully met the requirements with the exception of the intermodulation product level. With signals of +50 dBm and +20 dBm, the IM signal could not be reduced below -40 dBm. While this is sufficient to lessen the problem of intermodulation product generation, it does not meet the desired IM levels.

4. The primary achievement of this effort is an improved understanding of the generation of intermodulation products in a ferrite. In addition, a tunable UHF isolator for the frequency range 225 to 400 MHz was designed and built with a power handling capability of 100 watts and with a 20 dB isolation bandwidth of 4.3 to 7.6 percent.

5. To significantly reduce intermodulation product generation in a lumped circulator will require a breakthrough in the materials used in the circulators. Until such a breakthrough in materials occurs, no further development of this device is planned.

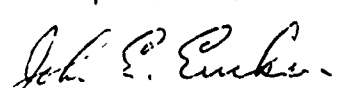

JOHN E. ERICKSON
Project Officer

TABLE OF CONTENTS

LIST OF ILLUSTRATIONS

SECTION I

INTRODUCTION

This is the final report on Contract F30602-71-C-0222. The object of this program was to develop a means of reducing the intermodulation signal products generated in collocated transmitters operating in the 225 to 400 MHz frequency range. Two such collocated +50 dBm transmitters operating with individual antennas isolated by 30 dB can produce intermodulation signal levels of 0 dBm. These intermodulation signal levels can render communications channels useless over a range of at least 20 miles. Conventional filtering can reduce the intermodulation products to the -70 to -80 dBm level for signals displaced in frequency by 1 or 2 percent.

The original goal of this program was to significantly reduce the intermodulation level for signals with essentially zero frequency separation. The intermodulation reduction technique was to cover the 225 to 400 MHz band and, if possible, have an extended frequency coverage.

The design goal IM reduction was to be accomplished by cascading four tunable isolators and a standard filter with each transmitter (Figure 1). The initial efforts were therefore focused on the development of the tunable circulator.

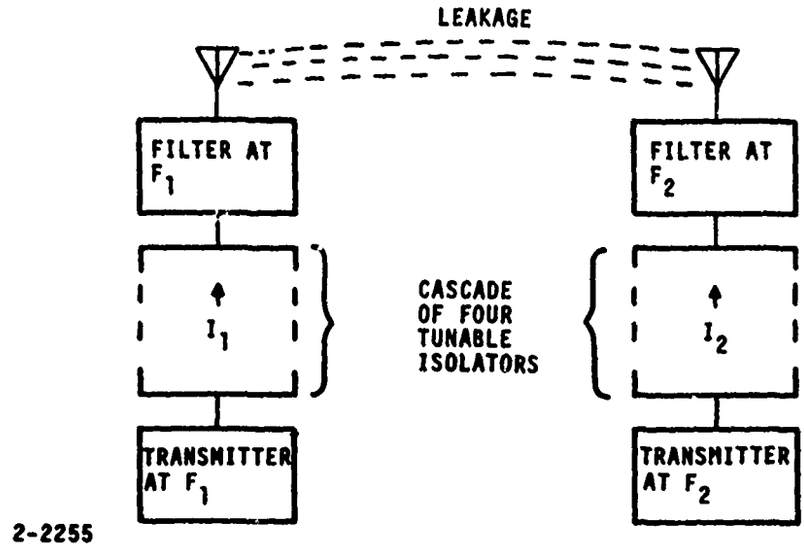

Figure 1---Schematic Diagram of Intermodulation Reduction Technique

A tunable, compact lumped-parameter circulator was developed to cover the entire 225 to 400 MHz band with a typical forward loss of 0.5 dB, and a 20-dB isolation bandwidth of 6 percent. The power handling substantially exceeds the 100-watt level, but the intermodulation level is only -40 dBm for a transmitter power of +50 dBm and an interfering signal of +20 dBm. Although this is well short of the -70 to -80 dBm objective, the tunable lumped-parameter circulator still represents a significant accomplishment applicable to this program and other Air Force requirements. In addition, there is a reasonable possibility that lower IM levels could be realized.

Although the widely tunable lumped-parameter circulators would substantially reduce the interference range, they would not supply sufficient protection for collocated receivers and transmitters. The design goal IM reduction to the -70 to -80 dBm range is required for this application. In order to approach this level, attention was turned to larger, distributed type isolators. The best commercially available units of this type exhibit an IM generation of -60 dBm for the input levels of interest (+50 and +20 dBm). Although several different approaches to improving the IM characteristics have been investigated, the -60 dBm level has not yet been substantially bettered.

This report describes the development and measured data of the lumped-parameter isolator, as well as the efforts to reduce the IM generation in distributed type isolators.

SECTION II

HIGH POWER TUNABLE UHF ISOLATOR

During the first phase of this study program, a compact lumped-parameter tunable isolator was developed to cover the 225 to 400 MHz band. This device represented a means of achieving the required 80-dB antenna-to-transmitter isolation intermodulation in a relatively small package. The system design goal for the cascade of the four isolators of Figure 1 were: a net isolation of 80 dB over a nominal 4-percent minimum bandwidth to complement the rejection characteristics of a two-section band-pass filter; an overall insertion loss of less than 2 dB; an ability to operate at an RF power level of 100 watts; and tunability over the 225 to 400 MHz band. The design goals for the individual tunable isolators were: a nominal insertion loss of 0.5 dB; a 20-dB isolation bandwidth of 4 percent; and an operating RF power level of 100 watts.

Basic relationships for this type of isolator have been published (1-4) with the most pertinent being Konishi's design curves which bridged the gap between theoretical analysis and practical application. This work set down practical guidelines for the various isolator parameters, but did not specify the optimum combination of ferrite characteristics and physical construction. These guidelines were used to investigate various combinations of ferrite materials and isolator configurations resulting in a demonstration breadboard satisfying nearly all of the original design goals.

This section of the report will present the measured characteristics of this unit along with the design equations as derived from the literature, their application to this specific task, and a summary of the investigation of the lumped-parameter isolator in the UHF band.

1. DEMONSTRATION ISOLATOR

A lumped parameter isolator has been fabricated and has successfully demonstrated the ability of such a device to operate across the 225 to 400 MHz band. Figure 2 shows the isolator and Figure 3 shows the measured characteristics. The insertion loss is typically 0.5 dB, with the 20-dB isolation bandwidth ranging from 4.3 to 7.6 percent, which essentially satisfies the initial design goals set down for the individual isolators.

The variable capacitors in each arm are used to tune the isolator. The range of capacitance necessary to tune 225 to 400 MHz is 50 to 15 pF, and is achieved using a commercially available unit. These air variable capacitors consist of two 3 to 30 pF units joined at their center to form a 6 to 60 pF capacitor of twice the length.

2. DESIGN CONSIDERATIONS

The design of the lumped-parameter isolator considered its electrical performance in the UHF band and its ability to operate at an RF power level of 100 watts. The electrical design was carried out using the information contained in references 1 through 5.

Figure 4 shows the basic lumped-parameter isolator and Figure 5 shows the definition of pertinent dimensions. The design consists of determining the appropriate ferrite and coupling strip dimensions to match the ferrite properties to the desired frequency of operation. This was carried out through a series of experiments in which isolator characteristics were measured for various combinations of the two parameters. The results of this

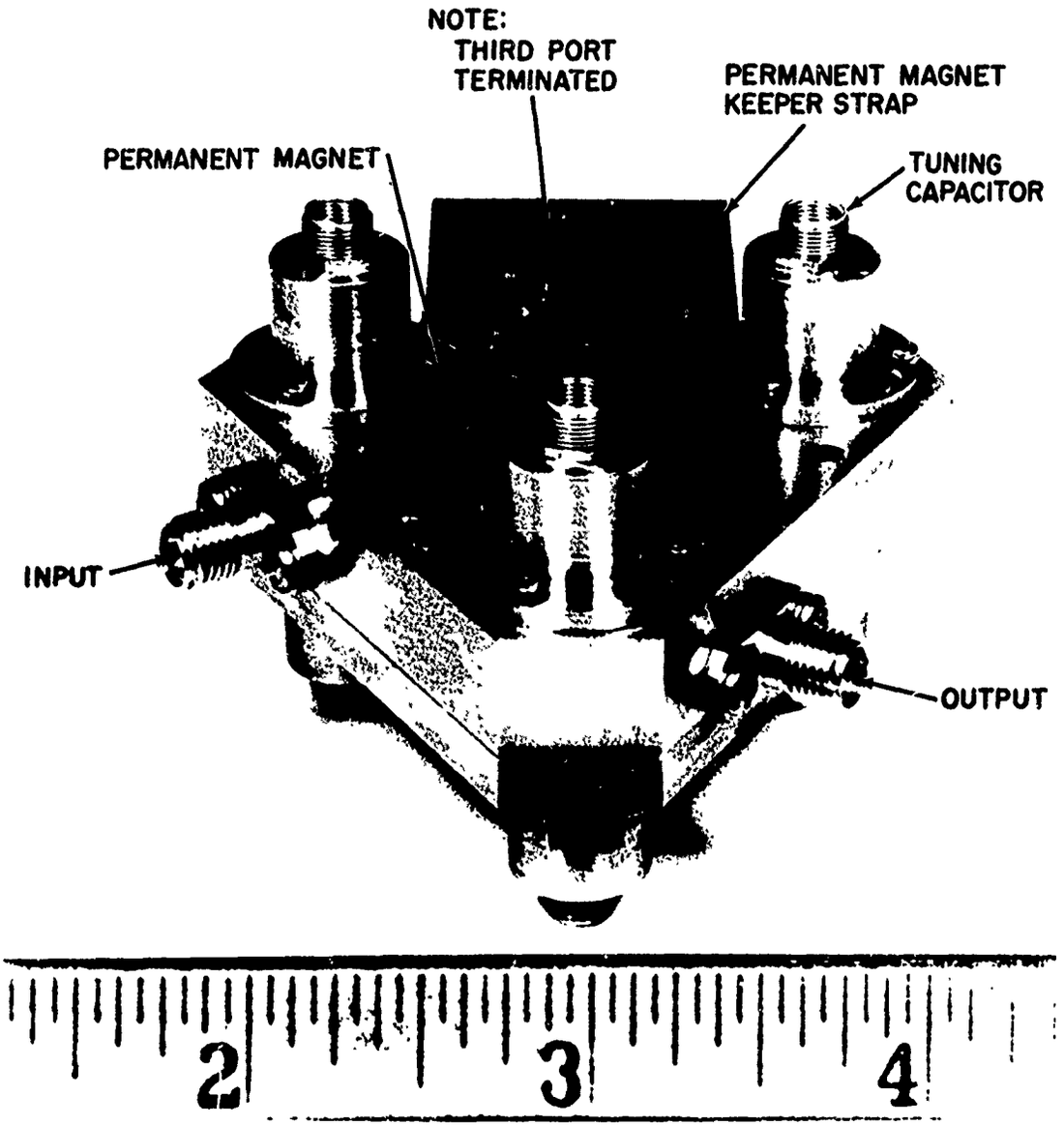

2-2256

Figure 2---Tunable UHF Isolator

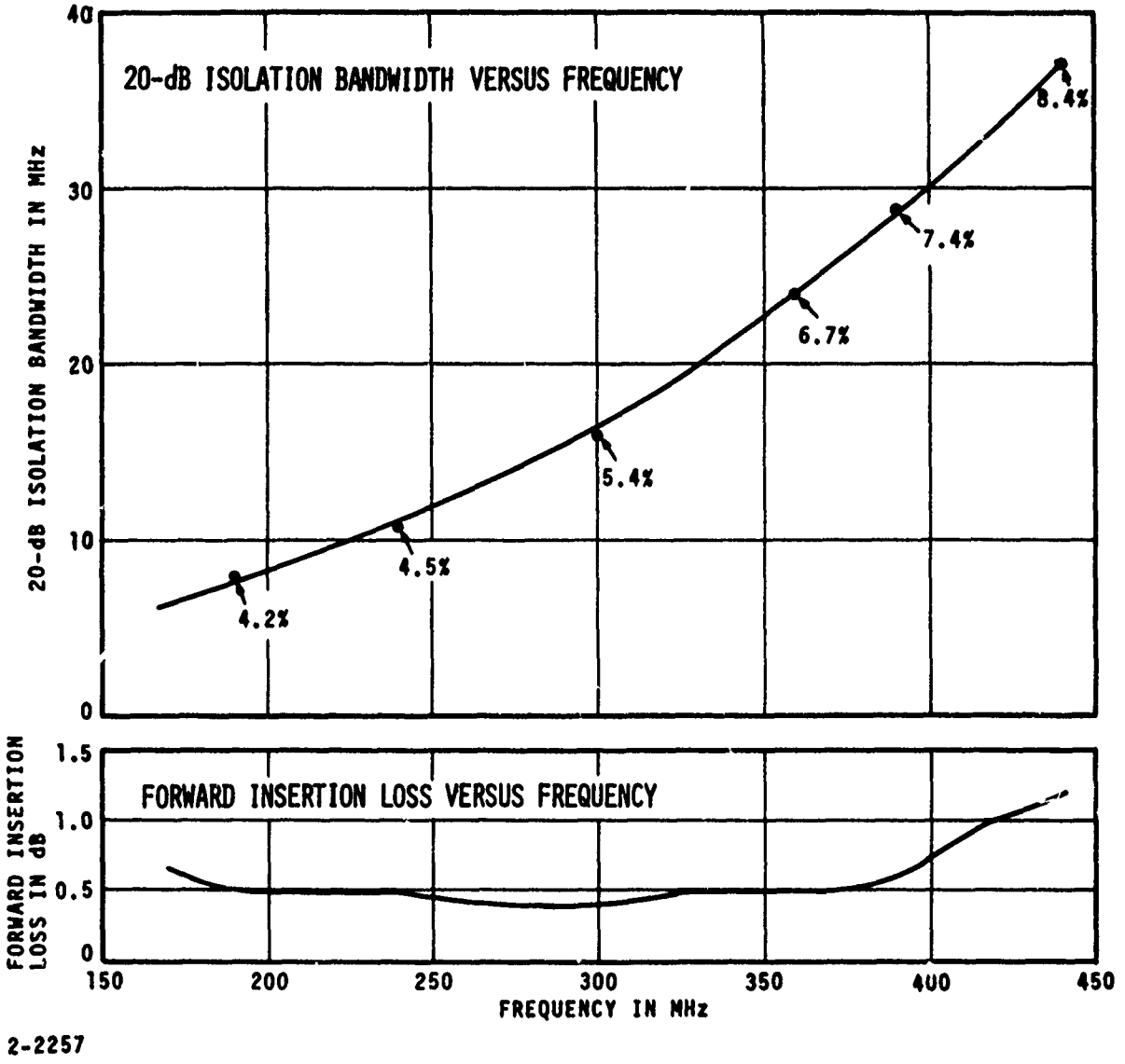

Figure 3---Measured Characteristics of UHF Tunable Isolator

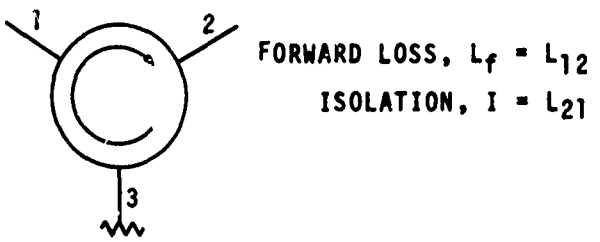

(a) ISOLATOR FORMED BY TERMINATED CIRCULATOR

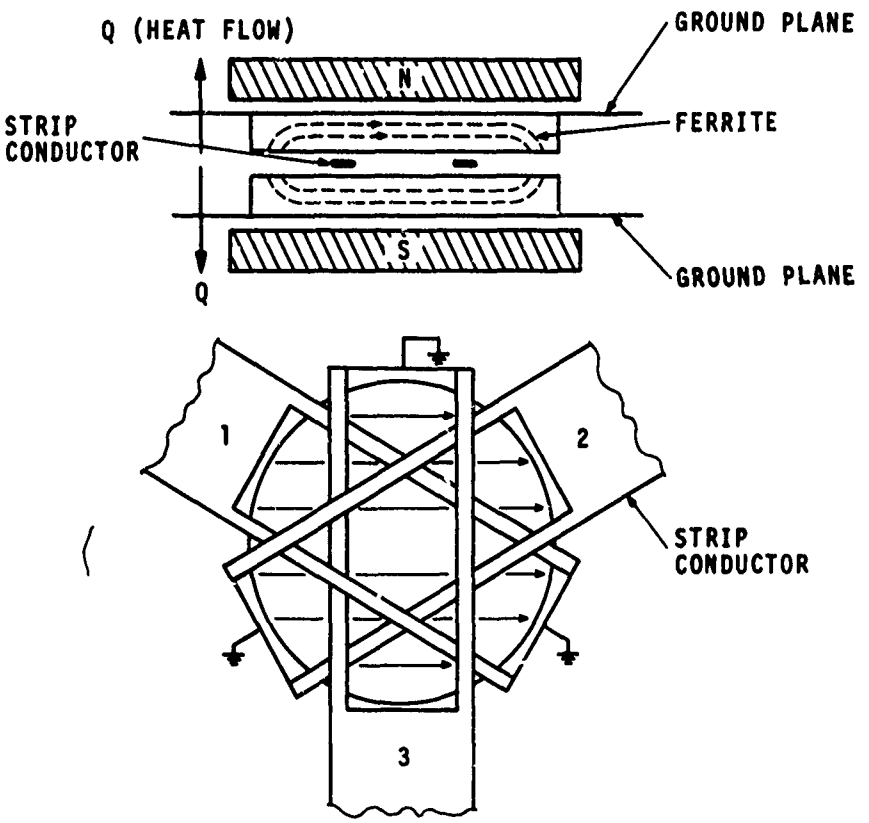

(b) CIRCULATOR CONSTRUCTION

0-5311

Figure 4---Basic Isolator

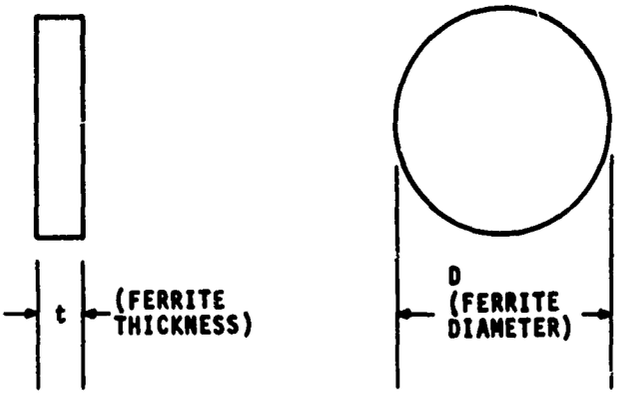

(a) DEFINITION OF FERRITE
MATERIAL DIMENSIONS

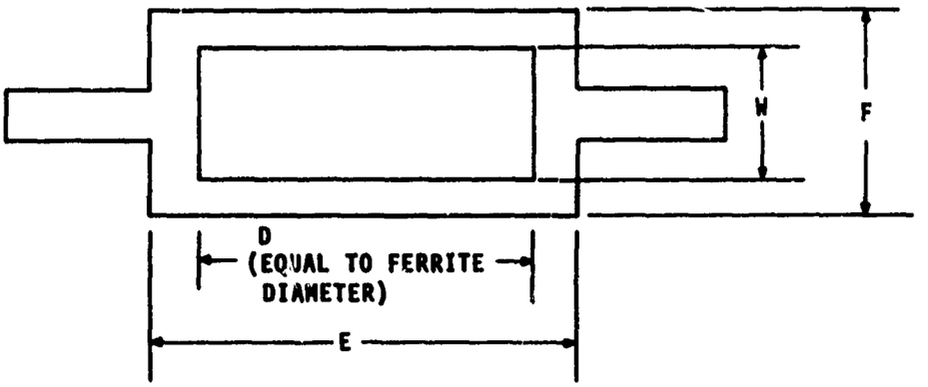

(b) DEFINITION OF COUPLING
STRIP DIMENSIONS

1-3460

Figure 5---Definition of Ferrite Material and Coupling

investigation, presented in Section 2.b.(2), represent a significant contribution to the practical realization of lumped-parameter UHF isolators. The net result, of course, being the isolator reported in the previous section.

This section will present the basic relationships describing the lumped-parameter isolator and the results of the investigation of the optimum design.

a. RF Properties

Design equations for the tunable UHF isolator have been derived from references 1 through 5. These equations are used to optimize the desirable electrical properties of the isolator:

- Minimum forward loss
- Isolation bandwidth
- Tuning range

The design equations have many terms in common. To simplify the presentation of these equations, a glossary of terms follows:

$4\pi M_s$ = saturation magnetization of ferrite material in gauss

ΔH = line width of ferrite material in oersted

γ = gyromagnetic ratio, constant = 2.8 MHz/gauss

H_0 = Kittel field, magnetic field internal to ferrite

$f_0 = \gamma H_0$ = Kittel resonance frequency in MHz

$f_m = \gamma 4\pi M_s$ = saturation magnetization frequency in MHz

N_t = demagnetizing factor in the x and y directions of the ferrite

f = operating frequency

ω = radian operating frequency

f_H = highest operating frequency

(1) Forward Loss

For the above resonance ferrite being employed, the Kittel resonance frequency, f_0, is set to a value which is greater than the highest operating frequency, f. The ratio σ is then defined as:

$$\sigma = \frac{f_0}{f} = \frac{\gamma H_0}{f} > 1 \qquad (1)$$

where σ is an independent design parameter. The useful range of σ for the isolator design lies between 2 and 5. Outside this range, the isolator performance deteriorates. As σ gets very close to 1 (the operating frequency approaching the Kittel resonance), the forward loss

of the isolator increases sharply; and, as σ gets very large (operating the isolator far below resonance), the isolation bandwidth decreases. The optimum value of σ for a particular ferrite material and operating frequency range is determined experimentally.

An approximate expression for the forward loss of the isolator, L in dB, as a function of σ is given as (2):

$$L = 2.5 \frac{\gamma \Delta H}{f} \left(\frac{\sigma^2 + 1}{\sigma^2 - 1} \right) \text{ dB} \tag{2}$$

An approximation to the forward loss due to the ferrite for operation far from resonance, $\sigma^2 >> 1$, is given as:

$$L \approx 2.5 \frac{\gamma \Delta H}{f} \text{ dB} \tag{3}$$

Equation 3 eliminates the functional dependence of forward loss on the ferrite resonance properties and illustrates the dependence of loss on the ferrite line width. Equation 3 indicates that to minimize the nonresonant loss properties of the ferrite material, the line width of the ferrite must be minimized. Unfortunately, it is not possible to use equations 2 or 3 directly to predict the forward loss because the value of ΔH is not known for the UHF band. The ΔH of ferrite materials is typically measured at 9 GHz and, while it is known that ΔH decreases with frequency, its final value in the UHF band is not known. The importance of equations 2 and 3 is that it indicates that ferrite materials with narrow line widths must be used to minimize the forward loss.

For a fixed ΔH and kittle field, H_0, combining equations 1 and 2 yields minimum loss for $\sigma = 2$, which is at variance with some of the experimental data (for example, Table II of the following section). The measured increase in forward loss with decreasing σ is accounted for by another important ferrite loss mechanism, low field loss. This occurs when the applied magnetic field is not large enough to fully saturate the ferrite, and the random orientation of the internal processing magnetic dipoles causes inefficient transfer of RF energy. Specifically, this occurs when

$$H_0 \leq N_t \, 4\pi M_s \tag{4}$$

and, therefore, to minimize low field loss, the inequality is reversed resulting in

$$H_0 \geq N_t \, 4\pi M_s \tag{5}$$

In terms of σ, equation 5 becomes

$$\sigma \left(\frac{f}{\gamma} \right) \geq N_t \, 4\pi M_s \tag{6}$$

The quantity $4\pi M_s$ is intrinsic to the ferrite, and N_t is determined by the geometric shape of the ferrite ($N_t \leq 0.15$ for the disc shape used in the isolator design). Equation 6 indicates that for a specific frequency of operation, low field loss is more easily avoided with large values of σ, which is at variance with the previous discussion in which $\sigma = 2$ is the optimum value for low forward loss. However, it is possible to choose ferrite materials with low values of $4\pi M_s$ and, thus, minimize the right-hand side of the inequality (equation 6) and allow values of σ to approach the optimum value of $\sigma = 2$.

In general, the appropriate value of σ and of $4\pi M_s$ for the specific frequency of operation is determined experimentally. For the UHF isolator developed for this program, this step in the design procedure is discussed in Section 4.d and summarized in Tables II, III, and IV.

(2) Isolation Bandwidth

The expression for the isolation bandwidth as given in reference 2, may be simplified by assuming $\sigma^2 >> 1$, and results in the following

$$BW\Big|_I = \frac{2\sqrt{3}}{I}\left[\frac{f_m (f)^2}{f_0 (f_0 + f_m)}\right] = \frac{2\sqrt{3}}{I}\left[\frac{f_m}{\sigma (\sigma + P)}\right] \tag{7}$$

where

$BW\Big|_I$ = isolation bandwidth at a given value of I

I = isolation level expressed as a power ratio

$P = f_m/f$

Equation 7 indicates that the isolation bandwidth increases with the frequency of operation or as it approaches the Kittel resonant frequency, $\sigma \rightarrow 1$. As for design criteria, it is seen that $BW\Big|_I \alpha 1/\sigma^2$, which suggests the use of low values of σ for optimum bandwidth.

(3) Tuning Range

The frequency of operation of the isolator is determined by the value of the effective inductance of the ferrite loaded coupling strips, ℓ, internal stray capacitance, and an external capacitor, Ce. Figure 6 shows a schematic diagram of the isolator.

At each frequency there is prescribed a capacitance and inductive value given by (1):

$$Ce = \frac{1}{\omega R_0}\left(\frac{f_0}{f}\right)\left[1 + \frac{f_0}{f_m}\right] = \frac{\sigma}{\omega R_0}\left[1 + \frac{\sigma}{P}\right] \tag{8}$$

$$\ell = \frac{\sqrt{3}\ \frac{R_0}{\omega}\ P}{(\sigma + P)^2 - 1} \tag{9}$$

where

Ce = external capacitance plus internal stray capacity

ξ = effective inductance

R_0 = external load resistance

The expression ξ is fixed by the property of the ferrite geometry, coupling strips, and ferrite RF characteristics and, thus, the frequency of operation of the isolator is adjusted by varying the external capacitor.

b. Thermal Properties

Maximum operating temperature of a ferrite device is related to the curie temperature of the ferrite. At the curie temperature, the spontaneous magnetization goes to zero and the isolator no longer acts as a nonreciprocal device. To avoid this problem, the ferrite material will be maintained at a temperature that is less than one-half its curie temperature. The ferrite materials used have curie temperatures ranging from 170 to 280°C and, therefore, operating temperatures of 85 to 140°C. As a safety factor, the maximum operating temperature of the ferrite was chosen as 60°C.

(1) Thermal Analysis

The ferrite temperature rises due to the RF power dissipated in the ferrite slabs. The total dissipated power is determined by the input power and forward insertion loss; it is assumed that this power is evenly divided between the two ferrite slabs. The power flow is from the plane of the coupled inductance strips, through the ferrite and the aluminum ground plane, and finally into the surrounding air. Figure 4 shows this situation.

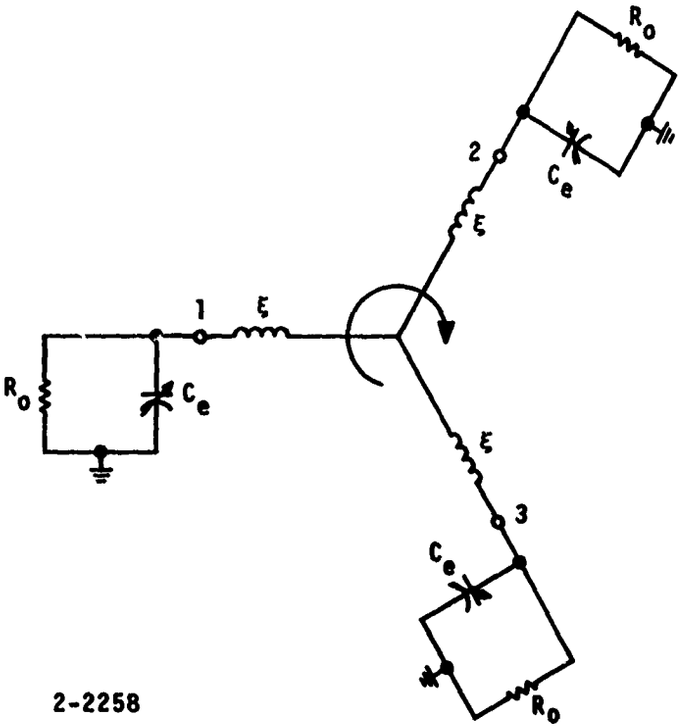

Figure 6---Equivalent Circuit of Tunable Isolator

The temperature rise across the ferrite is given by (6)

$$T_F = \frac{q\,\Delta X_F}{k_F\,A_F} \tag{10}$$

where

ΔT_F = temperature rise across the ferrite in ^{o}C

q = one-half the power dissipated in the isolator in watts

ΔX_F = thickness of ferrite slab in cm

k_F = thermal conductivity of ferrite in watt $cm/cm^2\ ^{o}C$

A_F = area of ferrite = $\pi D^2/4$

The temperature rise of the aluminum housing above ambient is given by (6)

$$\Delta T_H = \frac{q}{A_H}\,\frac{1}{h} \tag{11}$$

where

ΔT_H = temperature rise of housing above ambient in ^{o}F

q = one-half the power dissipated in the isolator, Btu/hr

A_H = one-half the total radiation and convection area of housing in ft^2

h = air transfer coefficient in Btu/hr $ft^2/^{o}F$

A nominal insertion loss of 0.5 dB implies that 12 watts will be dissipated by the isolator for 100 watts of incident power. Using equation 10 with

q = 6 watts

ΔX_F = (0.040 in.) (2.45 cm/in.) = 0.102 cm

k_H = 0.042 watt $cm/cm^2\ ^{o}C$

$A_F = \pi D^2/4 = \pi (0.6)^2/4$ in.$^2 \times (2.54)^2/$in.$^2 = 1.82\ cm^2$

results in

$\Delta T_F = 8^{o}C$

The maximum operating temperature of the ferrite is set by the temperature of the housing plus ΔT_F. The maximum value of T_H is

$$T_H = 60^{o}C - \Delta T_F \tag{12}$$

$$= 52^{o}C$$

Using an average value of the air transfer of h = 2.5, the area of the housing necessary to maintain this maximum temperature is calculated from equation 11.

$$A_H = \frac{q}{\Delta T_H} \frac{1}{h} \tag{13}$$

with

$$q = 6 \text{ watts} = 20.5 \text{ Btu/hr}$$
$$\Delta T_H = 52^{\circ}C - 24^{\circ}C = 28^{\circ}C = 50.5^{\circ}F$$

then

$$A_H = \frac{20.5}{50.5} \frac{1}{2.5} = 0.162 \text{ ft}^2 = 23.4 \text{ in.}^2$$

(2) Test Results

While the results of the thermal analysis indicated that an isolator with a total surface area of 46.8 in.^{2} would be required, the initial thermal testing was carried out using the test housing of Figure 7, which has a surface area of 25 in.^{2}. At an RF power level of 65 watts and 0.5-dB forward insertion loss, the isolator housing temperature rose 34°F from 74 to 108°F. This is approximately half the rise calculated for this housing and power level, 61°F. Reconsideration of the thermal analysis indicated that the value chosen for h was conservative and a more efficient air transfer coefficient of h ≈ 5 would account for this lower temperature rise. The conclusion that may be drawn is that the thermal analysis gives a range of rises for a range of values of h and, through experiments, the appropriate value of h has been determined.

It was concluded that the surface area of the isolator is to be approximately 25 in.^{2} to maintain the ferrite temperature less than 60°C for 0.5-dB forward loss and 100-watt RF input power.

3. THERMAL DEPENDENCE OF APPLIED MAGNETIC FIELD

A change in operating temperature results in a detuning of the isolator due to the temperature dependence of the ferrite properties. The value of the ferrite $4\pi M_s$ typically decreases with increasing temperature, and a decrease in the applied magnetic field is required to maintain the operating frequency. This may be seen by referring to equations 14 and 15 (Page 15) in which the interdependence of the isolator parameters is expressed algebraically. A set operating frequency implies f and σ are constants, which, from equation 15, requires H_0 to be a constant. From equation 14 it is seen that with a decreasing value of $4\pi M_s$ (temperature increasing), H_A, the applied magnetic field, must decrease to maintain H_0

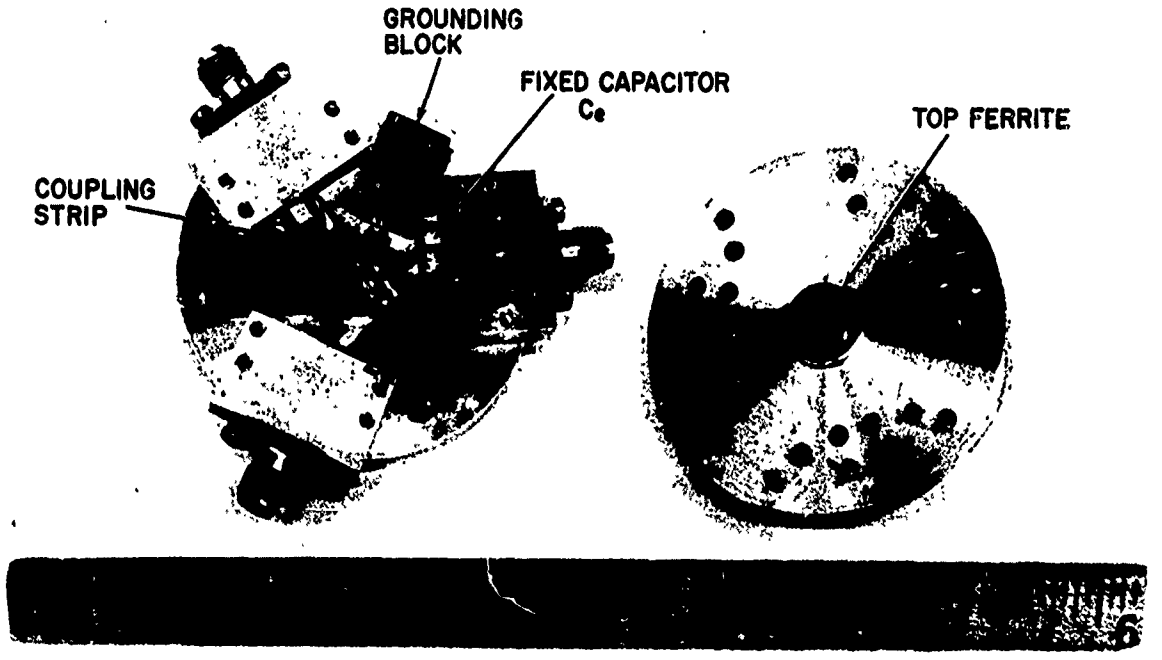

Figure 7---Lumped Parameter UHF Isolator Test Fixture

There is, thus, an additional thermal consideration for high power operations, that of temperature stabilization. This would be carried out by elevating the temperature of the isolator with an external heater to a value slightly above the level determined by the operating power. A temperature sensor would then be used to stabilize the isolator at the elevated temperature to compensate for the changes in RF power level. While the need for temperature compensation was recognized, its implementation was relatively simple in principle and represented an unnecessary level of product development for this study program. For the many high RF power tests carried out during IM evaluations, it was only necessary to adjust the bias field to compensate for the heating of the RF power.

4. DEVELOPMENT RESULTS

The development phase of the isolator design sought to determine the relationship between the design parameter σ and the ferrite $4\pi M_s$. For a particular ferrite material, an adjustable test fixture, shown in Figure 7, was used to set various values of σ in the 2 to 5 range, and the resulting electrical characteristics are measured. Equations 8 and 9 were

used to design the isolator and resulted in a typical set of designs as shown in Table I.* Table I shows that the change in σ is affected by altering the thickness of the ferrite and the value of the tuning capacitance, Ce.

The measured results of three ferrite materials covering the range of commercially available values of $4\pi M_s$ are reported: YIG with a $4\pi M_s$ of 1780 gauss; G-1010 with a $4\pi M_s$ of 1000 gauss; and, YAF-29 with a $4\pi M_s$ of 600 gauss.

Table I. Summary of Isolator Design Parameters for σ Ratios of 2, 3, 4, and 5, and an Operating Frequency of f = 312 MHz

$\sigma = \frac{\gamma H_0}{f}$	Ce (pF)	ξ (nH)	Ferrite Dimensions (in.) t	D	Coupling Strip Dimensions (in.) W	E	F
2	17.5	2.04	0.048	0.400	0.080	0.480	0.160
3	20.0	1.8	0.040	0.400	0.080	0.480	0.160
4	39.6	1.58	0.032	0.400	0.080	0.480	0.160
5	52.0	1.41	0.028	0.400	0.080	0.480	0.160

a. YIG Ferrite

High operating temperatures were initially expected and dictated the desirability of using YIG ferrite with its high curie temperature of 280°C. Table II presents the results of the measured characteristics of a YIG ferrite isolator for σ's of 2, 3, 4, and 5.

At each value of σ and Ce, optimum isolation and minimum loss do not coincide but are obtained at two different values of applied magnetic field. Peak isolation and higher loss are obtained with the lower value of applied magnetic field, whereas minimum loss and lower peak isolation are associated with the higher value of applied magnetic field.

The lack of coincidence between minimum loss and maximum isolation may be due to low field loss and is explained as follows. If low field loss is ignored, minimum resonance loss will theoretically occur at $\sigma = 2$. However, at this σ, low field loss is encountered and can only be avoided by decreasing the $4\pi M_s$ of the ferrite material or by raising σ.

The term σ can be raised in the following manner:

$$H_0 = H_A - \left(\frac{3N_z - 1}{2}\right) 4\pi M_s \tag{14}$$

$$H_0 = \sigma\left(\frac{f}{\gamma}\right) \tag{15}$$

---

* An illustrative example of this design procedure is carried out in Appendix I.

Table II. Measured Isolator Characteristics Using YIG Ferrite Material for Design σ's of 2, 3, 4, and 5

		Field Adjusted for Maximum Isolation				Field Adjusted for Minimum Forward Loss			
σ	Ce (pF)	f (MHz)	Forward Loss (-dB)	20-dB Isolation Bandwidth (percent)	Peak Isolation (-dB)	f (MHz)	Forward Loss (-dB)	20-dB Isolation Bandwidth (percent)	Peak Isolation (-dB)
2	15	407	2.3	*	24	453	1.2	*	20
	27	289	2.0	*	20	312	0.7	*	17
	58	190	1.0	*	18	199	0.7	*	14
3	15	425	2.0	16.0	35	476	0.8	9.9	23
	27	292	2.0	11.4	33	320	0.7	6.8	22
	58	186	1.4	7.2	>35	196	0.8	5.0	24
4	15	481	0.7	11.7	33	502	0.5	7.7	24
	27	327	0.8	8.7	>35	345	0.6	5.7	24
	58	207	1.0	5.0	35	218	0.8	4.0	23
5	15	490	1.4	-	35	520	0.4	-	23
	58	215	0.8	4.5	35	222	0.7	2.8	23

* Peak isolation too low to obtain meaningful bandwidth measurements.

Substituting equation 11 into 10, we obtain:

$$\sigma\left(\frac{f}{\gamma}\right) = H_A - \left(\frac{3N_z - 1}{2}\right) 4\pi M_s \qquad (16)$$

From equation 16 it can be seen that the value of σ is proportional to the applied field, H_A. As H_A is increased, σ will increase and the low field loss as expressed by equation 6 should be reduced. Associated with this reduction in loss is a decrease in peak isolation. This is due to the circulator operating at a σ that differs from that of the design σ. At higher design values of σ, the low field loss problem is minimized, but does exist.

These tests with YIG ferrite have shown that low field loss contributes significantly to a deterioration in the isolator's performance. YIG was considered because of its high curie temperature; however, subsequent tests with high power showed that the isolator's temperature rise was lower than expected. Therefore, ferrite materials with lower values of $4\pi M_s$ and curie temperature were next considered.

b. G-1010 Ferrite

The use of pure YIG having a $4\pi M_s$ of 1780 gauss contributes to an increase in low field loss and does not give optimum performance. The effect of low field loss was reduced by using G-1010 with a lower $4\pi M_s$ of 1000 gauss.

The isolator of Figure 7 was used to set four different values of σ for the G-1010 ferrite material and evaluated each at discrete frequencies with the use of fixed capacitors. Table III presents the measured isolator characteristics for two applied field conditions.

Except for $\sigma = 2$, Table III indicates that the isolation bandwidth varies inversely with σ, and is very similar in value to that obtained with YIG ferrite. For $\sigma = 2$, the bandwidth is at variance with that predicted theoretically and is not readily explainable. Minimum loss and peak isolation have both been improved by the use of G-1010 ferrite. The minimum loss has decreased from 0.7 to 0.5 dB, and the peak isolation has increased from 35 to 45 dB.

The most significant performance improvement obtained with the use of G-1010 material was achieved in obtaining good coincidence between maximum isolation and minimum loss. For $\sigma = 5$, Table III indicates that a 0.05-dB deterioration in loss was obtained when the magnetic field was adjusted for maximum isolation. This result is most probably attributable to the decreased low field loss due to the lower $4\pi M_s$ ferrite material being used. This result substantiates the idea proposed in the preceding section that reducing the value of $4\pi M_s$ of the ferrite would reduce the loss and improve the coincidence between minimum loss and maximum isolation.

c. YAF-29 Ferrite Material

A significant improvement was obtained in the circulator characteristics by decreasing the value of the ferrite $4\pi M_s$ from 1780 to 1000 gauss. To determine whether this trend of

Table III. Measured Isolator Characteristics Using G-1010 Ferrite Material for Design σ's of 2, 3, 4, and 5

		Field Adjusted for Maximum Isolation				Field Adjusted for Minimum Forward Loss			
σ	Ce (pF)	f (MHz)	Forward Loss (dB)	20-dB Isolation Bandwidth (percent)	Peak Isolation (dB)	f (MHz)	Forward Loss (dB)	20-dB Isolation Bandwidth (percent)	Peak Isolation (dB)
2	28	275	1.4	4.2	21	291	0.7	*	18
3	28	280	2.2	11.2	27	311	0.7	*	21
4	28	329	1.0	8.6	45	342	0.7	4.8	23
5	28	352	0.6	7.3	45	360	0.5	4.5	23

* Peak isolation too low to obtain meaningful bandwidth measurements.

improved circulator characteristics would continue with the use of an even lower $4\pi M_s$ material, circulators employing YAF-29 ferrite material with a $4\pi M_s$ of 600 gauss were tested and evaluated. Four values of σ were tested at discrete frequencies with the use of fixed capacitors. The measured results of the isolator performance, presented in Table IV, demonstrate a pattern of low forward loss and coincidence for values of σ other than $\sigma = 2$. The change in performance with $\sigma = 2$ suggests the limits of the design; the following discussion will focus on the useful design, that is, $\sigma = 3$, 4, and 5. The measured results of the isolator performance are significantly different from the two previous materials in that with the YAF-29 material coincidence was obtained between minimum forward loss and peak isolation for three of the four values of σ tested. This result was interpreted as an indication of an optimum combination of ferrite material and frequency of operation, and is directly attributable to the lower $4\pi M_s$ of YAF-29. It is this material with a design $\sigma = 3$ at the center of the band that was used to produce the tunable isolator reported in Section II.1 of this report.

As indicated in Table IV, a change in bandwidth characteristics has occurred with the use of YAF-29 ferrite. The ferrite materials previously tested had bandwidth characteristics that varied inversely with σ, while the bandwidths obtained with YAF-29 ferrite were independent of σ. The explanation of this characteristic is not found in Konishi's analysis, but does not represent a serious problem.

The use of YAF-29 ferrite has not changed the peak isolation and is still in the order of 40 dB or greater. Minimum loss, which had occurred at $\sigma = 5$ for the YIG and G-1010 ferrite, occurred at $\sigma = 3$ for YAF-29 ferrite. This substantiates the idea proposed that minimum loss should occur at approximately $\sigma = 2$ if low field loss was substantially reduced with the use of ferrite material with a low $4\pi M_s$.

Table IV. Measured Isolator Characteristics Using YAF-29 Ferrite Material for Design of σ's of 2, 3, 4, and 5

σ	Ce (pF)	f_c (MHz)	Forward Loss (dB)	20-dB Isolation Bandwidth (percent)	Peak Isolation (dB)
2	20	355.0	2.0	22.2	35
2	28	257.0	1.5	15.95	40
3	28	326.0	0.50	7.25	43
3	58	205.0	0.70	4.33	40
4	28	350.0	0.70	7.1	41
4	58	231.0	0.80	5.35	40
5	28	366.0	1.1	7.25	43
5	58	235.0	0.8	4.43	43
5	83	201.0	1.2	3.6	47

Note: Minimum loss and maximum isolation coincide at all σ's, except $\sigma = 2$.

d. Summary and Conclusions of Ferrite Material Investigation

The results obtained with YAF-29 indicate that coincidence bandwidth and loss characteristics are different from that obtained with YIG and G-1010 material. Table V presents a comparison of the characteristics of the three materials.

These results indicate that YIG material with a $4\pi M_s$ = 1780 gauss introduces higher loss and poor coincidence between minimum and maximum isolation. It therefore is not recommended for use in circulators operating in the 225 to 400 MHz region.

A comparison of the results obtained with the G-1010 and YAF-29 material indicates that YAF-29 ferrite has characteristics comparable to G-1010, which are considered acceptable. As a result, either ferrite could be used in designing a circulator in the 225 to 400 MHz region.

Though results with both types of ferrite were similar, coincidence occurred at all values of σ for YAF-29, implying that the effect of low field loss on coincidence and high loss at low σ's has been greatly reduced. If the line width, ΔH, of both materials had been the same, the reduction of low field loss would have resulted in a loss for YAF-29 lower than that obtained for G-1010. This did not occur, and it may be concluded that the ΔH of YAF-29 in the UHF band is greater than that of G-1010. The optimum material for use at UHF would be a material combining the $4\pi M_s$ of YAF-29 and the ΔH of G-1010.

Table V. Comparison of UHF Isolator Characteristics for Three Ferrite Materials

	YAF-29	G-1010	YIG
Bandwidth	Independent of σ	Varies Inversely with σ maximum at = 5	Varies Inversely with σ maximum at = 5
Minimum loss	0.5 dB at σ = 3	0.5 dB at σ = 5	0.7 dB at σ = 5
Coincidence between minimum loss and maximum isolation	σ = 3, 4, and 5	σ = 5	No coincidence

SECTION III

INTERMODULATION MEASUREMENT

The nonlinear behavior of ferrite when operated below resonance has been studied by Suhl (7). This work indicates that the onset of nonlinear high power effects in ferrite is a function of the ΔH and $4\pi M_s$ of the ferrite expressed as:

$$h\ (crit) = 1/2\ \Delta H \left(\frac{\Delta H}{4\pi M_s} \right)^{1/2} \qquad (17)$$

(equation 12-32, p 585, reference 5)

h (crit) = critical RF field, in oersteds, at which nonlinear effects take place

H = line width of ferrite material

$4\pi M_s$ = saturation magnetization of ferrite

Equation (17) indicates that to obtain a ferrite with high power handling capability, $4\pi M_s$ should be minimized and ΔH should be maximized. As ferrite loss increases with increasing ΔH, a compromise is needed in selecting a ferrite with a ΔH that yields low loss and a high h (crit).

1. MEASURED RESULTS

To ascertain the effect of ΔH and $4\pi M_s$ on IM levels, materials of different characteristics were checked. The value of σ chosen was optimum for the materials tested. With the circulator tuned with fixed capacitors, the frequency of operation, defining f_1, was 365 MHz for the YAF-29, G-1010 and G-1000 materials, and 311 MHz for YIG ferrite. The frequency of the interfering signal, f_2, was typically 10 MHz removed from f_1, which is within the bandwidth of the circulator in all cases. A listing of the materials and the corresponding measured results of IM level are presented in Table VI.

This data is at variance with the theory and indicated that a relatively constant IM level is obtained with materials of different $4\pi M_s$ and ΔH. A possible explanation for these results may be found in the above resonance operation of the circulator.

Equation (17) expresses the critical field level for a circulator operating at a high magnetic field and apparently does not apply to the above resonance operation being employed.

An experiment designed to ascertain the effect of ΔH on IM generation considered the use of nickel ferrite with an extremely large line width (ΔH) of 320 Oe. Unfortunately, due to the very large ΔH of nickel, very high loss was encountered and meaningful isolation and IM measurements could not be obtained with this material.

A comparison of IM characteristics of lumped parameter and distributed isolators taken for two orientations of interfering signals are presented in Table VII. For the reference measurement, both interfering signals enter the circulator at the same port and the measured IM level is dependent primarily on the ferrite material characteristics. The measurement setup is shown in Figure 8. For the operating measurement the signals are fed in at opposite ports simulating system operation. IM measured under this condition should indicate any improvement due to the nonreciprocal circulator properties. The measurement setup for operating condition is shown in Figure 9.

The results for the reference measurement of the lumped parameter circulator indicates that no substantial change in the IM level was noted for the ferrite materials presently being used. While the reference IM levels are comparable, a marked decrease in operating IM level was measured for the distributed type circulator* and not for the lumped type. The principal difference between the two types of circulators is their internal physical geometry. The difference in IM levels suggests that the physical configuration of the fields internal to the distributed type are such as to decrease the interaction of the interfering signals under operating conditions.

The decrease in IM level noted for the operating condition, while substantial, is not yet sufficient to satisfy the -80 dBm project goal. However, the realization that there is an inherent reference IM level (~ -40 dBm) that may be decreased through circulator geometry, is a major conclusion. Based on these measurements and conclusions, it is considered possible to develop an isolator that enhances the favorable geometry to produce a circulator with an IM level to meet the -80 dBm design goal.

2. MEASUREMENT TECHNIQUE

a. Measurement Setup

The measurement setups used for measuring IM levels under reference and operation conditions are shown in Figures 8 and 9. A calibrated Hewlett Packard spectrum analyzer is used to display the level of the $2f_1 - f_2$ IM signal frequency. This technique has a sensitivity of approximately -95 dBm when the analyzer IF bandwidth is reduced to 10 kHz. The increase in the analyzer sensitivity is proportional to the reduction in its IF bandwidth.

To reduce the levels of the f_1 and f_2 signals below the saturation level of the spectrum analyzer, multisection band stop filters tuned to f_1 and f_2 are inserted between the coupler and the analyzer. In this way the sensitivity of the analyzer may be maximized while avoiding any internally generated signals due to strong f_1 or f_2 signals.

b. Test Setup Calibration

A test signal at the intermodulation frequency (f_{IM}) of known amplitude is injected into the measurement setup at point A, and the deflections on the analyzer recorded. Point A is then reconnected into the system and the amplitude of $f_{IM} = (2f_1 - f_2)$ is then read from the calibrated screen of the spectrum analyzer.

---

* Addington Lab Model No. 113-0026A.

As mentioned previously, the sensitivity of the setup is approximately -95 dBm. However, the minimum measurable IM is -75 dBm as the f_{IM} signal is sampled through a 20-dB directional coupler. (The calibration f_{IM} test signal is injected directly into the setup at point A). To compensate for the directional coupler, +20 dB must be added to the amplitude of the f_{IM} calibration signal. Therefore, a -95 dBm calibration signal corresponds to a -75 dBm f_{IM} signal. The system sensitivity can be increased beyond the required -80 dBm by replacing the Hewlett-Packard spectrum analyzer with a test receiver or the AIL spectrum analyzer with its -110 dBm sensitivity.

3. CONCLUSION

From the measurement of the intermodulation product levels of the lumped and distributed parameter isolators, it was evident that a distributed isolator offers advantages. IM measurements were taken under two conditions:

- Both interfering signals feed into one port (reference)
- Signals feed into opposite isolator ports (operation)

For the distributed type isolator an improvement over the reference IM level on the order of the isolation was noted. The IM level decreased 20 dB from -40 dBm to -60 dBm. However, for the lumped parameter type isolator, no such improvement was measured. The explanation of this phenomenon is to be found in the difference of the geometry of the internal interacting RF fields between the two types of isolators.

Table VI. Measured Intermodulation Levels for Lumped Parameter Circulator with Interfering Signal Levels of +50 dBm and +20 dBm

Ferrite	$4\pi M_s$ (gauss)	ΔH (Oe)	Measured Level (dBm)
YAF-29 (AL-YIG)	600	30	-42
G-1010 (AL-YIG)	1000	40	-40
G-1000 (GD + AL + YIG)	1000	55	-35
G-113 (YIG) (Pure YIG)	1780	40	-38
TT_2-130 (Nickel)	1000	320	-----*

* No circulation action as large ΔH can give rise to large loss.

Table VII. Measured Intermodulation Levels of Lumped and Distributed Parameter Circulators For Interfering Signal Levels of +50 dBm and +20 dBm

	IM Level for Interfering Signals of +50 dBm and +20 dBm	
Lumped Circulator Ferrite Material	Reference Measurement (Figure 8) (dBm)	Operating Measurement (Figure 9) (dBm)
YAF-29	-42	-42
G-1000	-40	-40
G-1000	-35	-35
G-113	-38	-38
Distributed Circulator	-40	-60

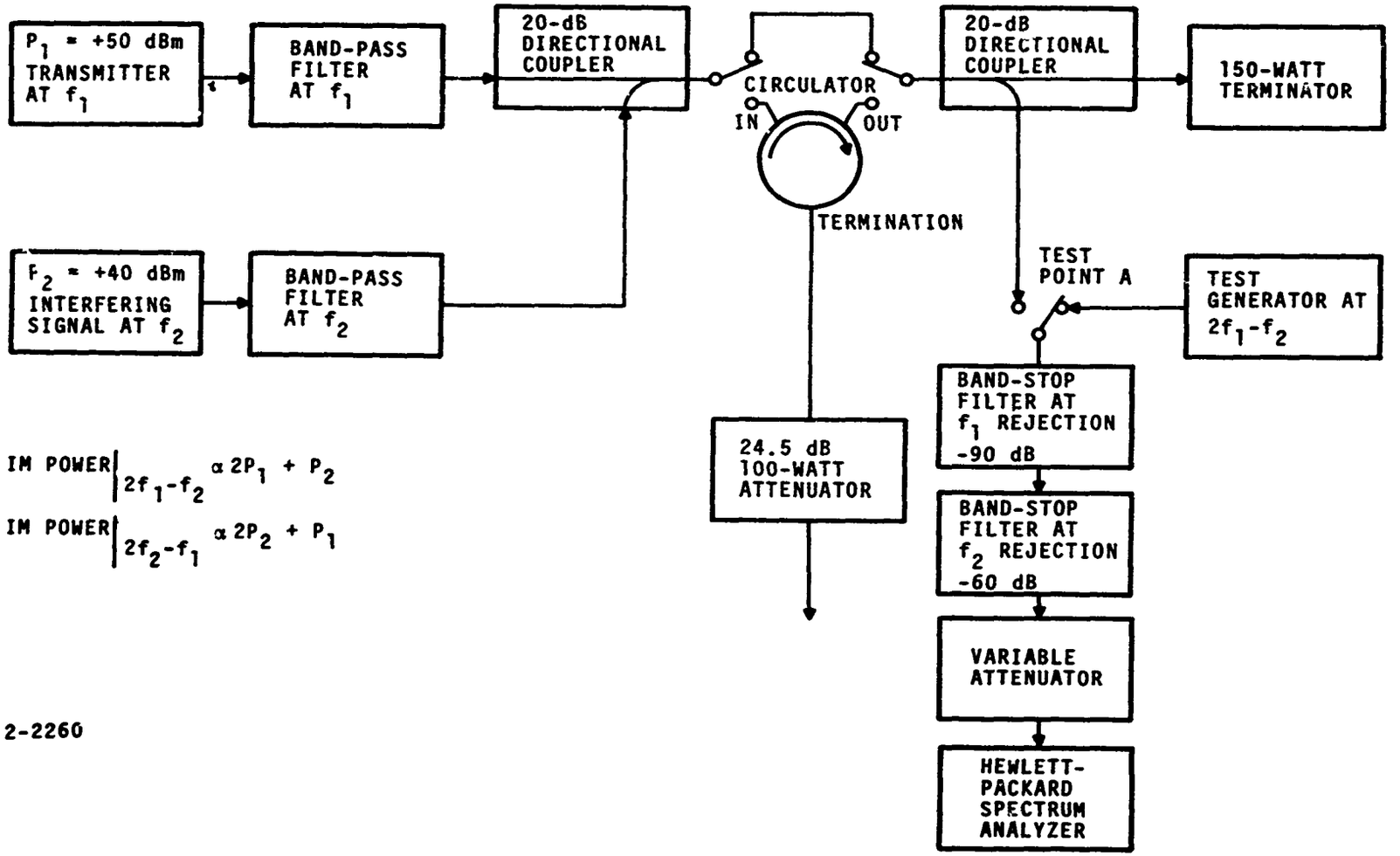

Figure 8---Intermodulation Measurement Equipment Setup; f_1 and f_2 in Same Circulator Port--Reference Condition

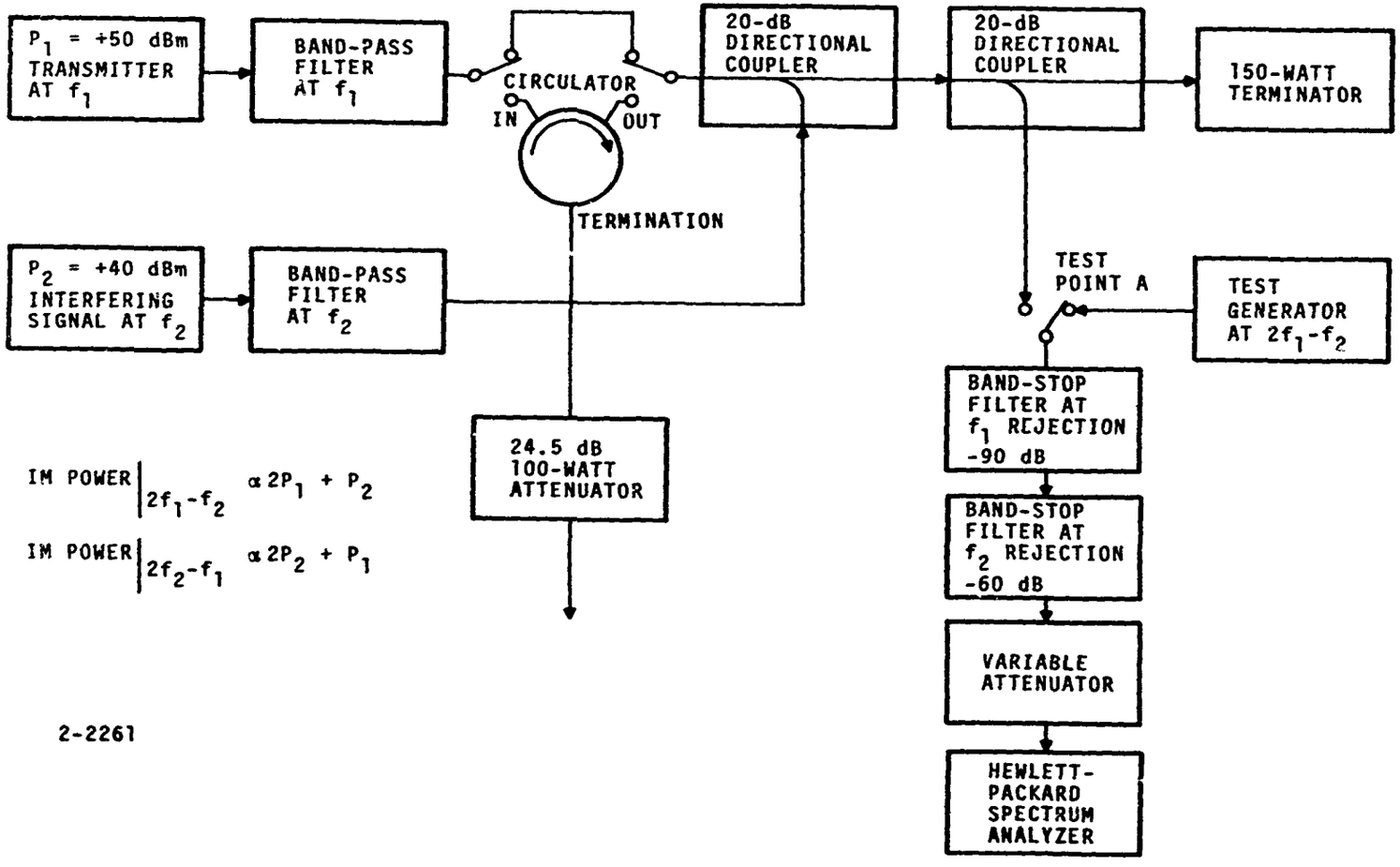

Figure 9---Intermodulation Measurement Equipment Setup; f_1 and f_2 in Opposite Ports--Operating Condition

SECTION IV

DISTRIBUTED ISOLATOR

1. INTRODUCTION

As explained in the previous section, the IM test data indicated that the distributed type circulator was more likely to meet the IM design goal than the lumped element type. These results necessitated a change of project emphasis to the distributed type. It was hypothesized that the mechanism of spatial separation associated with the distributed circulator could allow the possibility of achieving the reduction of the IM level to -80 dBm.

This section of the report presents a qualitative explanation of how the IM product level is related to the mechanism of spatial separation and a description of the distributed isolators designed to enhance the effects of spatial separation. Two basic types have been considered. The first increases the port-to-port angular separation from 120 to 180 degrees. The second employs an inhomogeneous applied field or inhomogeneous ferrite to provide two paths, one favoring low forward loss, the other favoring high isolation or field splitting.

2. SPATIAL SEPARATION WITHIN THE FERRITE MATERIAL

It is shown in Appendix II that the amplitude of third-order intermodulation term is given by $\rho A_2 A_1^2$ where ρ represents the nonlinearity of the material and A_2 and A_1 are the amplitudes of the weaker and the stronger interfering signals, respectively. As a ferrite isolator is a magnetic device the amplitudes will indicate the strength of the respective magnetic inductances so that $IM \propto B_2 B_1^2$.

The efforts toward lowering the level of intermodulation are based upon the fact that in a distributed device, it is possible to influence the spatial geometry of the fields in the bulk of the ferrite material. With this in mind, special methods are being explored to change the field geometry of B_2 and B_1 selectively so that they are influenced in a different way. Because of the nonreciprocity of the device and the fact that the two interfering signals enter at different ports, the validity of this concept is theoretically justified.

By achieving a spatial separation of the fields B_1 and B_2, the product of $B_2 B_1^2$ in any volume element of the ferrite will be decreased, resulting in a lower intermodulation level. A direct proof of the validity of this concept has already been demonstrated in the course of this program. It has been shown that in a three-port circulator of the distributed type a substantially higher IM level was measured in the case when both interfering signals entered at the input port as compared with the case when the interfering signals entered at input and output ports, respectively (refer to Table VII).

This effect was not present in the lumped type of circulator. This mechanism may be understood better by considering Figure 10.

Figure 10 is a representation of the three-port circulator. As indicated, most of the energy associated with B_1 tends to go to port 2 while a smaller amount will find its way to port 3. The same applies for the energy connected with B_2 with respect to ports 3 and 1.

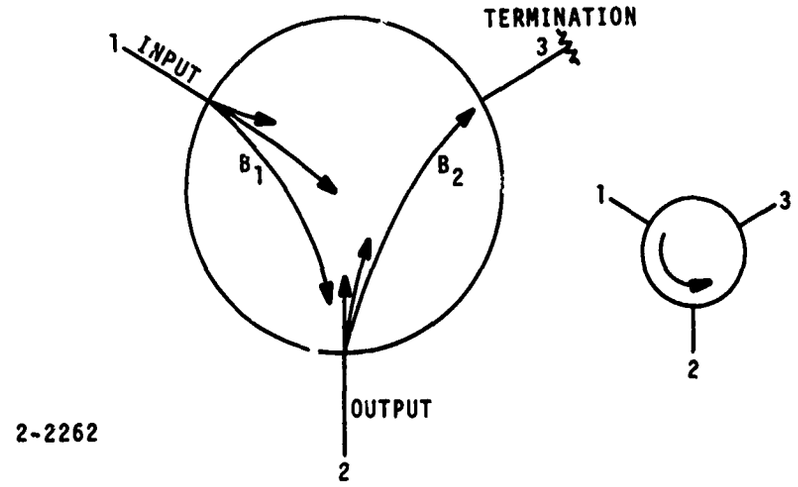

Figure 10---Energy Flow in a Three-Port Circulator

The higher the ratio of the amounts going to the wanted and unwanted ports, the higher "field splitting" is said to be present. For clairity, only the inherent field splitting is shown.

As can be seen from this model, the field splitting should be maximized in order to minimize the intermodulation. The principal means of maximizing field splitting are by optimizing the inner conductor geometry, and by using an inhomogeneous field or inhomogeneous material. Testing of both these techniques has been carried, with the results being described in the following subsections.

3. 180-DEGREE ISOLATOR

An isolator with 180-degree port-to-port separation, shown in Figure 11, was designed to improve the field splitting by geometric considerations. The reduction in the distributed circulator IM level obtained under system operation condition, implied that increasing the physical separation of the fields set up by the +50 and +20 dBm signal, and thereby reduce their interaction, will reduce the level of the IM product. This device represents the maximum possible separation, 180 degrees. As a result, it is no longer symmetrical for use as both an isolator and circulator as with a 120-degree separation, but interest is focused on a low IM isolator which does not require this form of symmetry.

YAF-29 ferrite was used in all the distributed designs. This choice was based on the results obtained with this material when used in the UHF lumped element circulator. Basic ferrite characteristics are independent of circulator configuration, and YAF-29 should be well suited for use in the distributed element circulator.

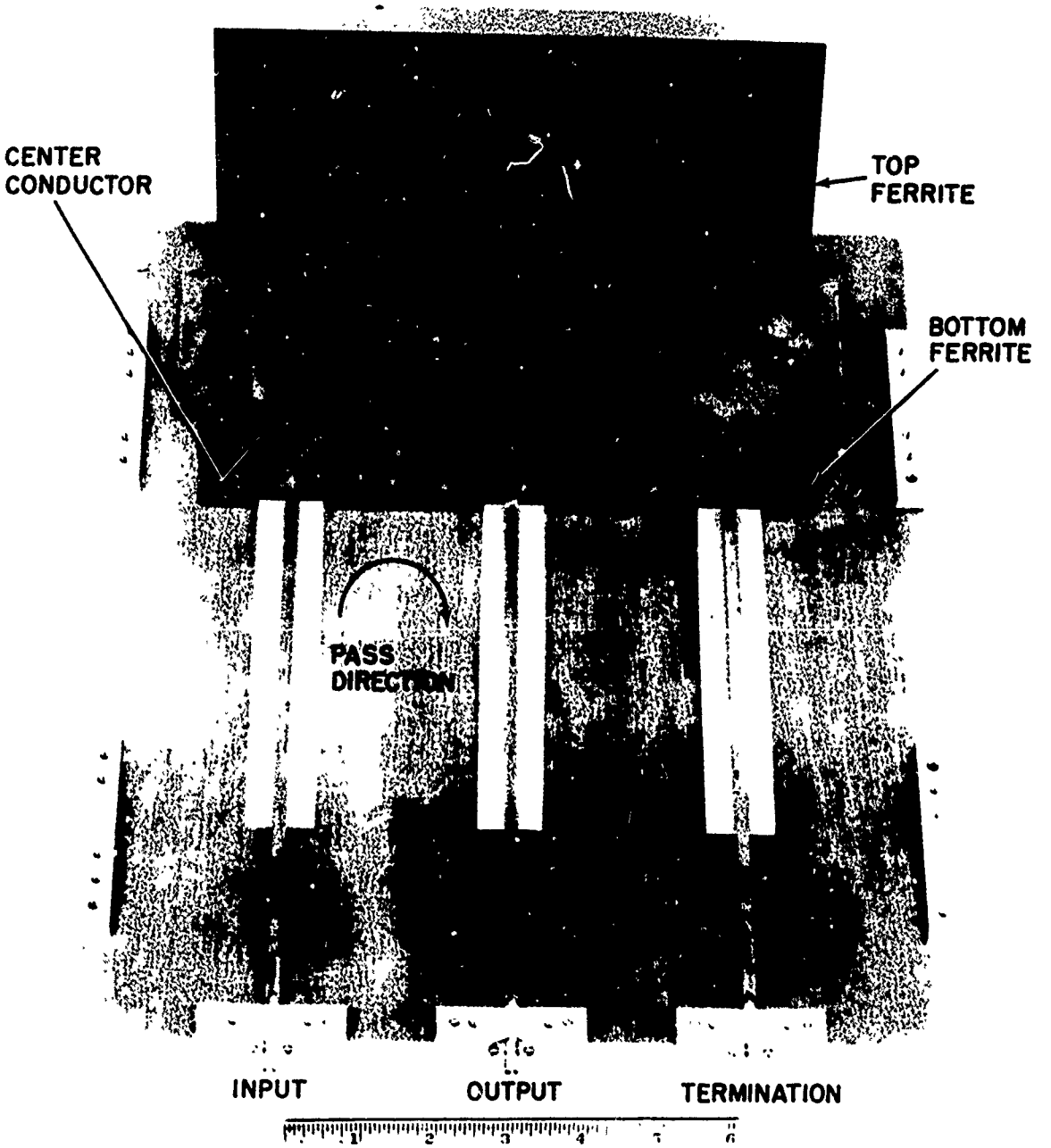

2-2263

Figure 11---UHF Isolator with 180-Degree Port-To-Port Separation

Measurements taken on the 180-degree isolator indicated that high splitting was not consistent with low forward loss. The unit exhibited about 4-dB forward loss for 20-dB isolation. The high forward loss stems from the fact that improved field splitting could only be achieved by adjusting the applied magnetic field to bias the ferrite close to magnetic resonance.

These measurements indicate that it was not possible to establish both low forward loss and high field splitting with geometric considerations only. Inhomogeneous conditions would have to be established in order to have the two desired field conditions realized simultaneously.

4. INHOMOGENEOUS APPLIED FIELD/FERRITE ISOLATOR

An inhomogeneous applied field or inhomogeneous ferrite results in an inhomogeneous internal field; one portion of the ferrite is biased higher or lower with respect to the rest. The higher bias implies operation further removed from resonance and lower forward loss; the lower bias field will result in the ferrite operating closer to resonance where enhanced field splitting is expected. By the proper distribution of the bias field, a relatively low loss path can be established for the transmit signal, and, at the port the transmit signal exits and the interfering signal enters, the field splitting between the two signals may be improved over homogeneous conditions.

The relationship between the internal field of the ferrite (H_0) and the applied field (H_A) is:

$$H_0 = H_A - (\text{constant}) \times (4\pi M_s) \tag{18}$$

For a uniform ferrite material ($4\pi M_s$ = constant), $H_0 \propto H_A$, and the control over H_0 is realized through the applied field. In this inhomogeneous applied field condition, the transmit path must have a larger field applied to it than the isolation path. For a uniform applied field (H_A = constant), H_0 increases or decreases when $4\pi M_s$ decreases or increases, respectively, and thus the transmit path must have a ferrite with a $4\pi M_s$ lower than that of the isolation path.

This section of the report presents the results of measurements taken on an isolator with an inhomogeneous applied magnetic field.

Inhomogeneous Applied Magnetic Field

A Y circulator using YAF-29 5-inch diameter ferrite discs (Figure 12) has been aligned to operate with an inhomogeneous applied magnetic field at approximately 310 MHz. Forward insertion loss was approximately 0.5 dB over an established 20-dB isolation bandwidth. The operating bandwidth of the isolator, while not optimized, was sufficient to make measurements of the IM generated for signals separated by 20 MHz.

The applied magnetic field was made inhomogeneous by inserting a semicircle of steel to enhance the field over approximately 1/3 of the ferrite area as shown in Figure 13.

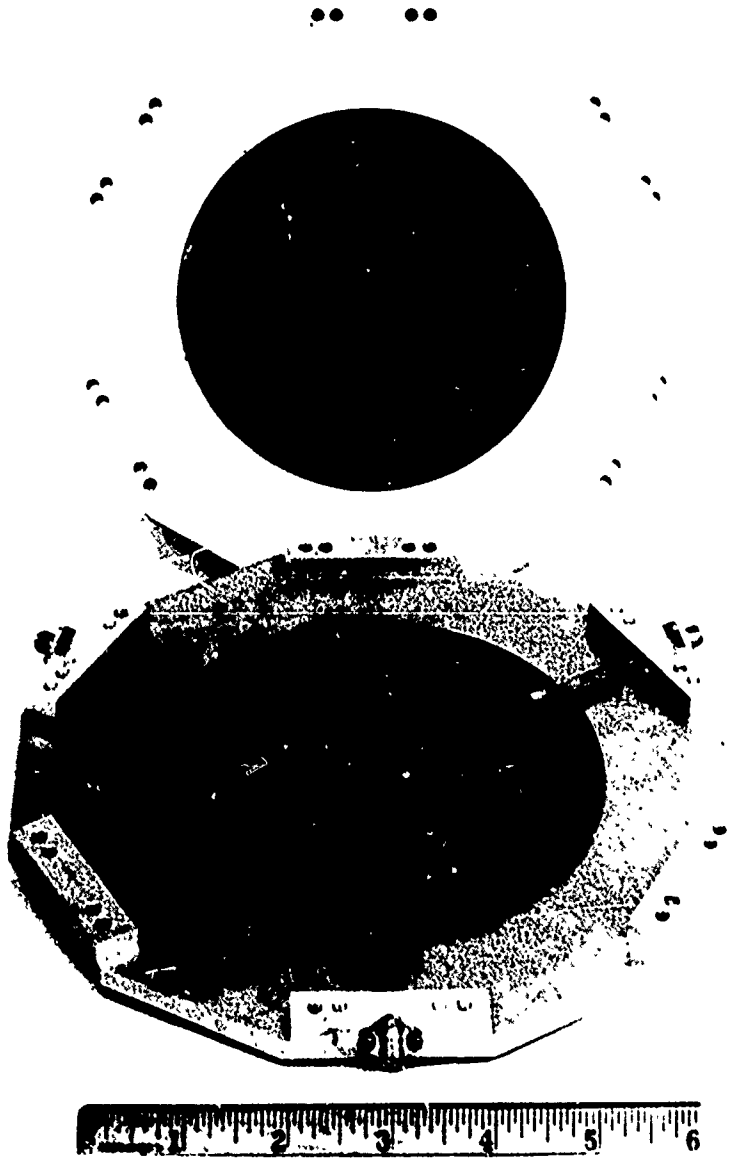

2-2264

Figure 12---Y Circulator Using YAF-29 5-Inch Diametric Ferrite Discs

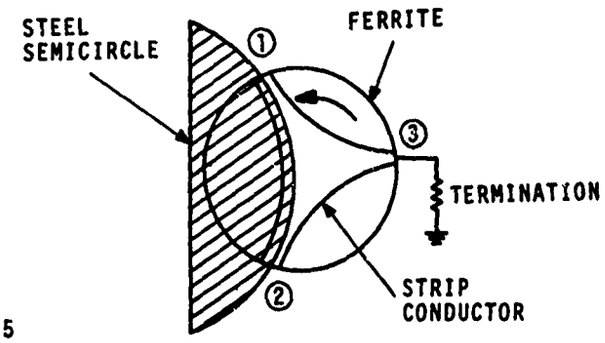

Figure 13---UHF Isolator with Inhomogeneous Applied Magnetic Field

With an overall uniform applied magnetic field, the field under the area of the steel semicircle will be larger than that biasing the remaining ferrite. In this way the forward loss path, (1) to (2), will be operating further away from resonance to reduce the loss, while the isolation path, (2) to (3), biased at a lower field and closer to resonance, will experience an enhanced field splitting.

Measurements of IM levels under these conditions give levels of -60 to -65 dBm, comparable to the levels measured for homogeneous applied magnetic field. A well-defined boundary between the high and low applied field regions most probably did not exist in the ferrite and is the most likely explanation of the lack of IM improvement. The enhanced field splitting is dependent upon the establishment of such a condition. The use of a homogeneous applied field and inhomogeneous ferrite will result in a better defined high and low operating region and will represent a more accurate test of the field splitting thesis. The testing of the inhomogeneous field case was carried out first, since it was a relatively simple alteration of the Y circulator orginally fabricated.

SECTION V

PHENOMENOLOGICAL DESCRIPTION OF GENERATION OF INTERMODULATION PRODUCTS IN FERRITE CIRCULATORS

During this program an analysis was made of the intermodulation products that could be expected as a result of the nonlinear behavior of ferrite at high power levels.

Following common practice the output amplitude was represented as a function of the input amplitude by means of a power series with constant coefficients

$$V_0 = \alpha_1 V_i^1 + \alpha_2 V_i^2 + \alpha_3 V_i^3 \ldots\ldots + \alpha_n V_i^n$$

Assuming an input amplitude consisting of two in-band signals at different frequencies, $V_i = V_1 \cos \omega_1 t + V_2 \cos \omega_2 t$ whereby for the purpose of this program it can be assumed that $V_1 >> V_2$. It is found (Appendix II) that if the power series is truncated after three terms a third-order intermodulation product is generated:

$$\frac{3}{4} \alpha_3 V_2 V_1^2 \cos (2\omega_1 - \omega_2) t$$

If the strong amplitude V_1, associated with the +50 dBm signal, is modulated, that is $V_1 = V_1 (1 + m \cos \omega_m t)$, where m = modulation depth and ω_m is the angular modulation frequency, it is found that the modulation of the strong signal is carried over to some extent onto the weak signal (cross modulation). The amount of cross modulation is usually expressed in the cross-modulation factor $\frac{m_c}{m}$ where m_c is the induced modulation depth on the weak signal.

This ratio is given by $\frac{m_c}{m} \approx 3 \frac{\alpha_3}{\alpha_1} V_1^2$. As for a low-loss passive device, $\alpha_1 \approx 1$ and $\frac{m_c}{m} \approx 3 \alpha_3 V_1^2$.

Substituting this value into the expression found for the third-order intermodulation term yields:

$$V_{\text{intermod}} = \frac{1}{4} \frac{m_c}{m} V_2$$

so that a fixed relation exists between the cross modulation and the amount of third-order intermodulation.

Based on this principle, a measurement setup was devised that enabled the measurement of the cross modulation with a sensitivity corresponding to an intermodulation level of ≈ -90 dBm when the two input signal powers were +50 and +20 dBm, respectively.

This was a much higher sensitivity than could be obtained with a direct spectrum analyzer measurement at the intermodulation frequency.

Performing the measurement with the above mentioned signal levels, no cross modulation could be observed indicating an IM level lower than -90 dBm. However, a direct spectrum analyzer measurement showed an IM level of ≈ -40 dBm.

After assuring, by various measurements, that the observed intermodulation was indeed generated in the circulator, the fact had to be faced that the measurements were incompatible with the theoretical results obtained from the power series approach.

Although, admittedly, taking into account more than three terms, a fixed relation between IM and cross modulation no longer exists. The absence of one while the other is present is impossible under various bias conditions, when analyzed under the power series approach (Appendix II).

It was at this point, that it was realized that the credibility of the power series approach is seriously challenged, if a feedback exists between output and input . In Appendix II it is explained that in a nonlinear network with a limited amount of isolation between input and output, theoretically an infinite number of harmonics will be generated regardless of the inherent degree of nonlinearity.

Moreover, a concrete example is analyzed, where it is shown that third-order intermodulation can be generated without the presence of cross modulation, when the inherent nonlinearity can be completely described by only two terms of a power series. In this case the amplitude of the third-order intermodulation term is proportional to the amplitude of the second harmonic that is generated.

This proportionality has indeed been observed in the measurements performed during this program.

CONCLUSIONS

Based on the measurements performed during this program, in conjunction with the analysis presented in Appendixes II and III, the following phenomenological statements seem to be justified:

- The inherent nonlinearity in a ferrite at high power levels, can be practically described by taking into account only second-order nonlinearity.
- Third-order intermodulation is being generated because of feedback phenomina (internal reflections, etc.) and is proportional to the generated amount of second harmonic.
- Cross modulation effects can be neglected.

These qualitative statements will constitute an important part of the knowledge upon which further experimental work in the area of intermodulation will be based.

SECTION VI

CONCLUSIONS AND RECOMMENDATIONS

A tunable lumped parameter isolator has been developed for the 225 to 400 MHz band to limit the intermodulation product generated in collocated Air Force 100-watt transmitters. Typical forward loss is 0.5 dB with a 20-dB isolation bandwidth ranging from 4.3 to 7.0 percent. The objective of -70 to -80 dBm maximum IM level generated by the transmitters can be achieved by cascading four such isolators (Figure 1) to provide a minimum of 80-dB isolation to interfering signals. IM measurement of the isolators under the worst case RF power level conditions of +50 dBm main signal and +20 dBm interfering signal, experienced by the isolator closest to the antenna, indicated IM levels of -40 dBm.

While the initial design goal of -80 dBm IM level cannot be met, based on the -40 dBm level, the interference problem experienced without such isolator protection would be improved. Referring to Figure 1, the filters shown are those referred to in the work statement that would provide 70-dB attenuation at a frequency separation of about 2 percent. The isolators are the lumped parameter units with 20-dB isolation each for a total of 80 dB. For this combination, the IM level at the transmitter output would always be below -80 dBm. The IM problem area would now be transferred to the isolator receiving the highest interfering signal level, the one closest to the antenna. This would be at most -40 dBm (an improvement of 40 dB as compared to no isolators) and would reduce the 20-mile interfering range to 0.2 mile. In addition, if the filter used with these isolators was able to provide 70-dB attenuation to frequencies displaced by 2 percent, it would provide about 35-dB attenuation at a separation of 1 percent. This attenuation level, in conjunction with the isolator IM level, would result in an overall IM output of -75 dBm.

In summary, when compared with communication systems protected only by filters, the filter-isolator combination would reduce the IM interference range from 20 to 0.2 mile for closely spaced transmitter frequencies and would provide -75 dBm IM outputs for frequencies separated by at least 1 percent.

A minimum IM level of -40 dBm was measured for the lumped parameter isolator, independent of the orientation of the interfering signals. This is in contrast to the results obtained for the distributed type isolator in which a decrease in IM level was noted when the signals entered the device at opposite ports. The possibility of reducing the IM level produced in a ferrite device by spatially separating the interfering signals was thus identified. The distributed isolator IM level is 20 dB lower (-60 dBm) through this mechanism, and efforts were made to enhance the separation by designing special distributed isolators. Two types have been tested; port-to-port separation increased from 120 to 180 degrees, and an inhomogeneous applied magnetic bias field used on a standard isolator with 120 degrees separation. While no substantial decrease below the -60 dBm level was noted for these two designs, a third design employing inhomogeneous ferrite in a standard 120-degree isolator is being pursued. It is realized that once an isolator is developed with an inherent IM level under operating conditions of less than -80 dBm, the requirement on the remaining isolators in the chain will be reduced by the isolation offered by the preceding unit. Thus, while there is one special low IM isolator required for any transmitter, it need be only one and the originally proposed IM reduction technique, based on the successful development of a low IM isolator, is a viable and practical approach.

Based on the realization that there is a requirement for only one low IM isolator to effectively provide IM protection down to -70 to -80 dBm levels, it is recommended that the

efforts to develop such a device be continued. Inhomogeneous ferrite and larger disc circuits should be investigated. The measured data and analytic information on IM production in UHF isolators presented in this report will act as a very effective starting point for the development of the required low IM isolator.

One interesting by product of this program is the development of compact, widely tunable isolators using lumped elements. Figure 14 shows the size reduction that has been attained relative to a standard distributed element approach. While these isolators produce -40 dBm IM levels for +50 and +20 dBm inputs, there are many system's applications that are emerging. Some examples are:

- Buffering between high-power UHF circuits such as transmitters and antennas
- High power SPDT switching
- A basic nonreciprocal element for the realization of UHF equalizer networks

It is recommended that RADC consider these applications as well as the low IM application in applying the technology developed on this program to future needs.

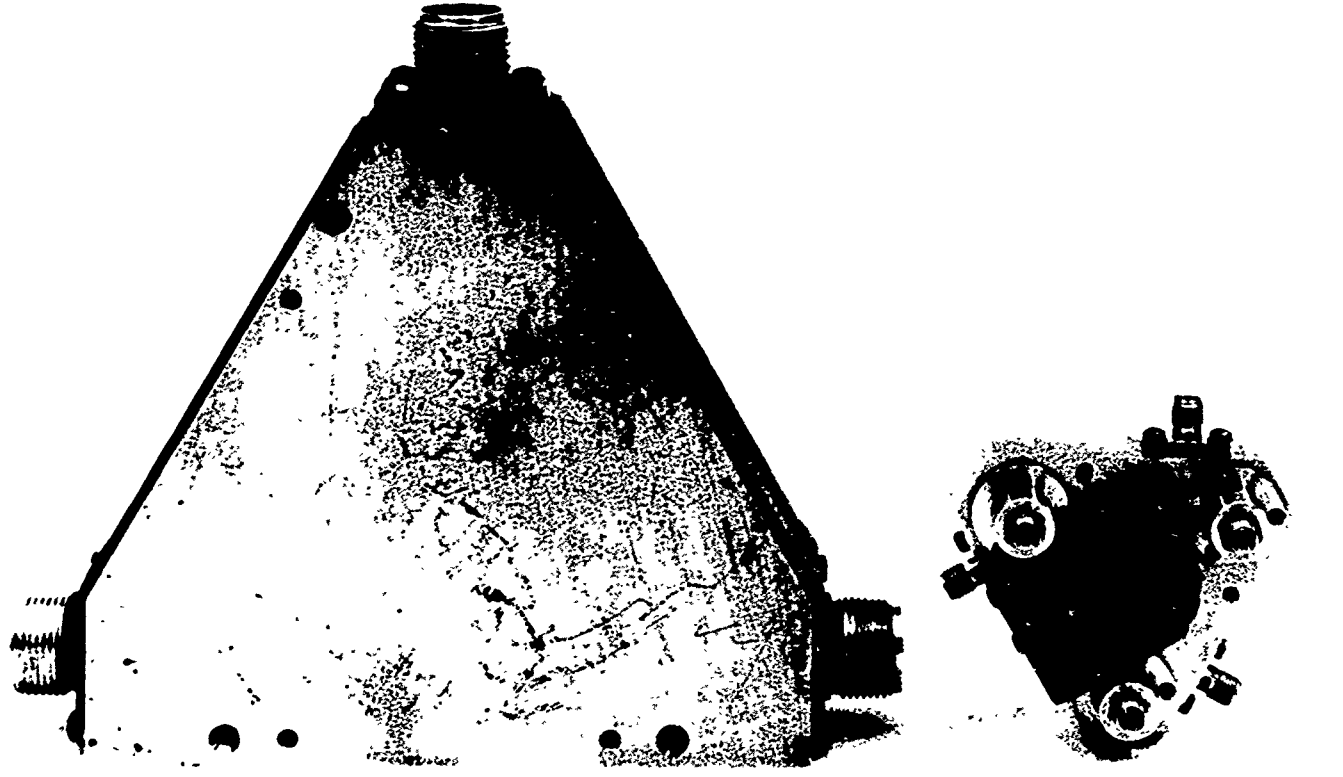

2-2266

STANDARD DISTRIBUTED CIRCULATOR

TUNABLE LUMPED PARAMETER CIRCULATOR

Figure 14---Tunable and Distributed Type UHF High-Power Circulators

SECTION VII

PAPER SEARCH

A computer-aided search of the DDC data bank on government suggested research, periodicals, and textbooks, related to the field of interest, was undertaken. In general, it has been found that the open literature on ferrite and circulators has been more useful than the classified government contract documents obtained from a computer-aided search of the DDC bank. Many entries were screened for pertinence to this program. Seven references have been of particular assistance, while 34 have been of general interest.

1. REFERENCES

1. Y. Konishi, "Lumped Element Y Circulator," IEEE Trans, Vol MTT-13, p 852-864, November 1965.

   The basis of VHF circulator technology.

2. R. Roberts and V. Dunn, "New Design Techniques for Miniature VHF Circulators," IEEE G-MTT Symposium Digest, Clearwater, Florida, May 1965.

   A companion early effort similar to reference 3.

3. Y. Konishi, "A High-Power UHF Circulator," IEEE Trans, Vol MTT-15, p 700-708, December 1967.

   Gives insight into performance of circulators under high power.

4. I. Rubinstein, "HF Tunable Circulators," IEEE Convention Record, New York, N.Y., March 1971.

   This is an interesting low-loss widely tunable circulator.

5. B. Lax and K. Button, Microwave Ferrites and Ferrimagnetics.

   A comprehensive textbook which will be helpful in assessing intermodulation effects.

6. "Heat-Flow Estimation," Electro-Technology, p 83-85, March 1965.

7. Suhl, "Nonlinear Behaviour of Ferrites at High Microwave Signal Levels," Proceedings of the IRE, p 1270-1287, October 1956.

2. BIBLIOGRAPHY

Aitken, F.M., and McLean, R., "Some Properties of the Waveguide Y-Circulator," Inst EE Proc, Vol 110, p 256-60, February 1963.

Bolt, F. D., "Four Simultaneous Transmissions From One Aerial; (the BBC VHF, FM transmitting station and Sandale, Cuberland). Electronic Eng, Vol 31, p 169-70, March 1959.

Brogdon, A. M., "Five-Way Antenna Coupler," il. QST, Vol 42, p 42-3+, November 1958.

Cacheris, J. C., and Sakiotis, N. G., "Ferrite Components for UHF and Microwave Systems," Electronics, Vol 34, p 37-42, 2 September 1961.

Case, W. E., et al, "Ferrimagnetic Resonance In Polyscrystalline Ferrite and Garnet Disks at L-Band Frequencies," J. Res. Nat Bur Stand, Vol 68C, p 85-9, April 1964.

Clevenger, R. R., Jr., "Advances in Ferrite Technology," Am Cer Soc Bul, Vol 44, p 216-20, March 1965.

Cochardt, A., "Recent Ferrite Magnet Developments," J Ap Phys, Vol 37, p 1112-15, 1 March 1966.

Cohen, H. M., "Polycrystalline Magnetic Garnets," il. Bell Lab Rec, Vol 46, p 55-60, February 1968.

Comstock, R. L., "Magnetoelastic Coupling Constants of the Ferrites and Garnets, IEEE Proc, Vol 53, p 1508-17, October 1965.

Degan, J. J., "Microwave Resonance Isolators," il. Bell Lab Rec., Vol 44, p 124-8, April 1966.

Deutsch, J., and Maier, H. G., "Gyromagnetic Resonance of Ferrites and Garnets at UHF," Inst. Radio Eng. Proc, Vol 49, p 1443-5, September 1961.

Dixon, S. Jr., et al, "Ferromagnetic Resonance and Nonlinear Effects in Ferrites with Uniaxial Anisotropy," J Ap Physics, Vol 41, p 1357-8, 1 March 1970.

Dunn, V. C., "Ferrites: Circulators for VHF and Up," il. Electronics Vol 41, p 84-7, 25 November 1968.

"Ferrite Permanent Magnets," il. Mech Eng., Vol 89, p 60, June 1967.

"Ferrites Resist Temperature Effects," Product Eng, Vol 39, p 77, 22 April 1968.

Friedman, A. N., "Miniature Ferrite Nonreciprocal Device," J Ap Phys, Vol 38, p 1419-20, 1 March 1967.

Graf, R. F., "Late Developments in Capacitor Design," Electronic Ind, Vol 24, p 70-3+.

Gyorgy, E. M., and Schnettler, F. J., "Induced Magnetic Anisotropy in Ferrite Single Crystals, J Ap Phys, Vol 35, p 1648-9, May 1964.

"Half-Inch YIG Filters Do Job of Three-Inchers," Electronics, Vol 39, p 99, 7 March 1966.

Hartwig, C. P., and Readly, D. W., "Ferrite Film Circulator," J Ap Phys, Vol 41, p 1351-2, 1 March 1970.

Heaton-Armstrong, L. J., and Jackson, B. S., "Modern Trends in High-Frequency Transmitter Design," il. Inst EE Proc, Vol 110, p 1385-94, August 1963.

Helszajn, J., "Simplified Theory of the Three-Port Junction Ferrite Circulator," Radio and Electronic Eng., Vol 33, p 283-8, May 1967.

Helszajn, J., and McStay, J., "Simplified Theory of Nonlinear Phenomena in Ferrimagnetic Materials," Inst EE Proc, Vol 114, p 1585-91, November 1967.

Hill, P. C. J., "Measurement of Reradiation from Lattice Masts at VHF," Inst. E.E. Proc, Vol 111, p 1957-68, December 1964.

Kumar, R. C., "S-Band Y-Junction Stripline Circulator with Triangular Ferrite," il. Electronic Eng, Vol 41, p 118-26, 3 March 1969.

Kuper, H., "Building an Antenna Coupler," Diags. QST, Vol 46, p 39-43+, February 1962.

"Medium-Power Bandswitching VHF Transmitter," QST, Vol 47, p 11-17, December 1963.

"New Developments in Ferrites," il. Ind Electronics, Vol 3, p 329, July 1965.

Norwood, M. H., "Voltage Variable Capacitor Tuning; a Review," IEEE Proc, Vol 56, p 788-98, May 1968.

Rowley, J., and Sheehan, E., "Design Considerations for Ferrite Junction Circulators," IEEE Proc, Vol 52, p 221, February 1964.

Seiden, P. E., and Grunberg, J. G., "Ferrimagnetic Resonance Linewidth in Dense Polycrystalline Ferrites," J Ap Phys, Vol 34, p 1696-8, June 1963

Sethares, J. C., and Purnhagen, T. G., "Anisotropic Spin-Wave Propagation in Ferrites," J Ap Phys, Vol 36, p 3402-4, November 1965.

Verweel, J., "Magnetic Properties of Ferrite Single Crystals with the Y Structure," J Ap Phys, Vol 38, p 1111-17, 1 March 1967.

Von Aulock, W. H., "Theory of Linear Ferrite Devices for Microwave Applications," J Ap Phys, Vol 37, p 939-46, 1 March 1966.

APPENDIX I

CIRCULATOR DESIGN PROCEDURE FOR $\sigma = 3$ AND $f = 312$ MHz

Using equation 1, we obtain

$$\gamma H_o = \sigma f_H \tag{19}$$

Let

$\sigma = 3$

f_H = highest operating frequency = 400 MHz

then

$\gamma H_o = 3 \times 400$ MHz = 1200 MHz

To avoid low frequency loss, equation 5 has to be satisfied.

$$\gamma H_o \geq \gamma N_t \, 4\pi M_s \tag{20}$$

Let

$N_t = 0.15$

then

$$4\pi M_s \leq \frac{\gamma H_o}{\gamma N_t} = \frac{1200}{2.8 \times 0.15} = 2860$$

The ferrite material to be used is pure YIG, with a $4\pi M_s$ of 1800 gauss. Though a material with a higher $4\pi M_s$ can be used, YIG has the advantage of having a relatively low loss coupled with a high curie temperature of 280°C.

To solve for Ce at an operating frequency of f = 312 MHz, we use equation 8 and obtain:

$$Ce = \frac{1}{\omega R_o}\left(\frac{f_o}{f}\right)\left(1 + \frac{f_o}{f_m}\right) \tag{21}$$

For

$\omega = 2\pi(312)$ MHz

$R_o = 50$ ohms

$f_o = \gamma H_o = 1200$ MHz

$f = 312$ MHz

$f_m = \gamma 4\pi M_s = 2.8 \times 1800 = 5000$

Then

$$Ce = \frac{1}{6.48 \times 312 \times 106}\left[\frac{(1200\ \text{MHz})}{312\ \text{MHz}}\right]\left[1 + \frac{1200\ \text{MHz}}{5000}\right] \tag{22}$$

$$Ce = 28\ \text{pF}$$

To obtain the effective inductance we use equation 9 and obtain:

$$\xi = \frac{\sqrt{3}\,\frac{R_o}{\omega}\,P}{(\sigma + P)^2 - 1} \tag{23}$$

where

$P = f_m/f$, $\sigma = f_o/f$

ξ = effective inductance

$$P = \frac{5000\ \text{MHz}}{312\ \text{MHz}} = 16.1$$

$$\sigma = \frac{1200\ \text{MHz}}{312\ \text{MHz}} = 3.84$$

$$\xi = 1.731\,\frac{\frac{50\,(16.1)}{2\,(312 \times 108)}}{(16.1 + 3.84)^2 - 1} = 1.8 \times 10^{-9}\ \text{henrys} \tag{24}$$

where ξ is 1.8 nH.

From Figure 15 (reference 1, p 855, Figure 2), we find that for a ξ of 1.8 nH that we have three choices of ferrite and coupling strip geometry.

The geometry that allowed for the most mechanically practical ferrite thickness (that is, the largest) was chosen for fabrication. The resultant dimensions are:

t = 0.040 inch

d = 0.400 inch

w = 0.080 inch

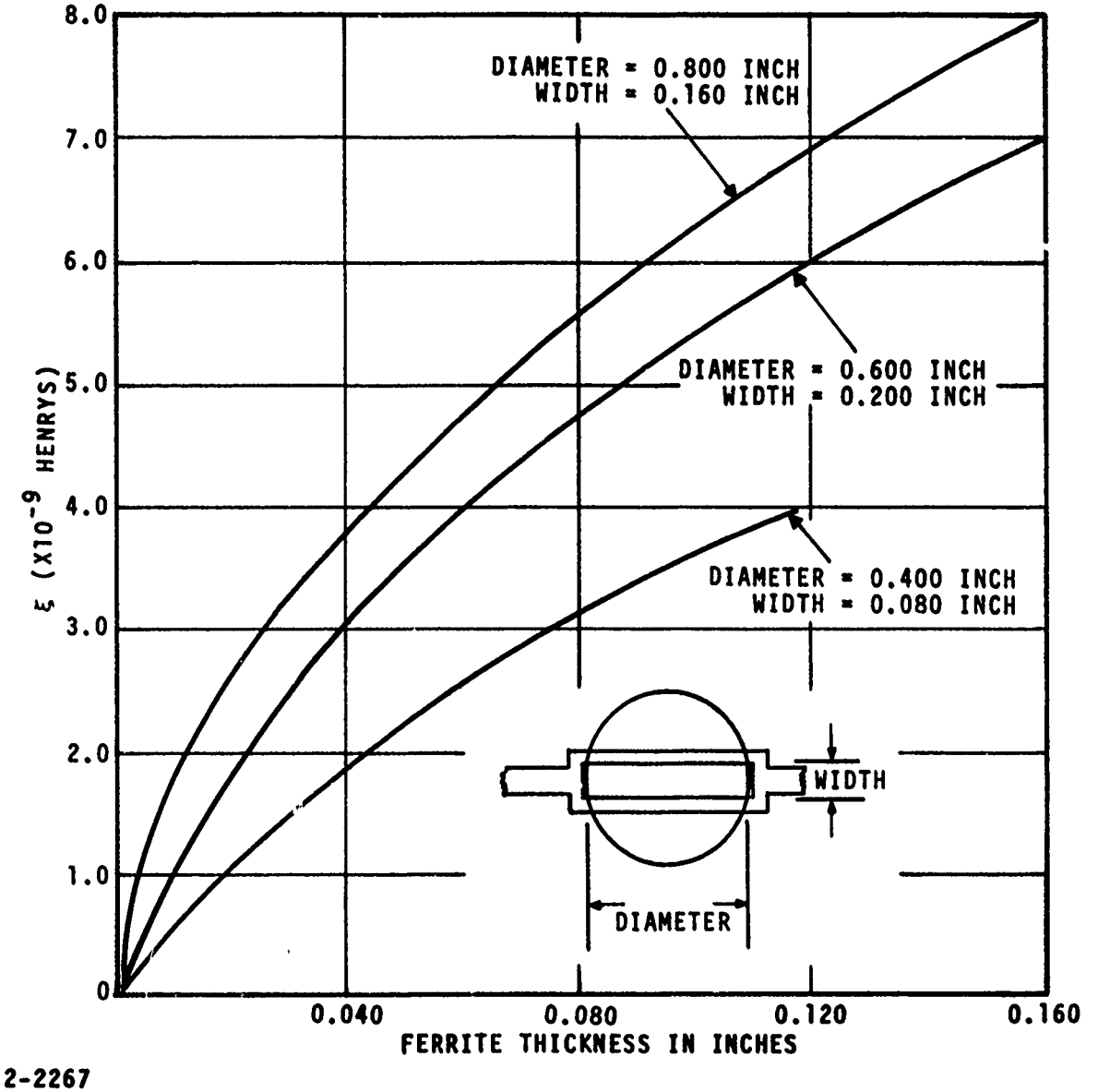

Figure 15---Measured Values of ξ Versus Ferrite Thickness

APPENDIX II

ANALYSIS OF INTERMODULATION AND CROSS-MODULATION PRODUCTS WITH THE GENERAL POWER SERIES METHOD

Let the output amplitude, V_o, as a function of the input amplitude, V_i, of a device be given by:

$$V_o = \sum_{n=1}^{\infty} \alpha_n V_i^n \tag{25}$$

where α_n is the constant coefficient of the n^{th} term

Let

$$V_i = V_1 \cos \omega_1 t + V_2 \cos \omega_2 t \text{ with } V_1 >> V_2$$

Then

$$V_o = \sum_{n=1}^{\infty} \alpha_n \left(V_1 \cos \omega_1 t + V_2 \cos \omega_2 t \right)^n$$

or

$$V_o = \sum_{n=1}^{\infty} \alpha_n \left(\sum_{p=0}^{\infty} \frac{n!}{p!\,(n-p)!} V_1^{n-p} \cos^{n-p} \omega_1 t \, V_2^p \cos^p \omega_2 t \right)$$

With the general relation:

$$\cos^u X = \frac{1}{2^u} \sum_{r=0}^{u} \frac{u!}{r!\,(u-r)!} \cos (u - 2r) X$$

$$V_o = \sum_{n=1}^{\infty} \alpha_n \sum_{p=0}^{n} \frac{n!}{p!\,(n-p)!} \cdot \frac{1}{2^n} V_1^{n-p} V_2^{p} \left[\sum_{r=0}^{n-p} \frac{(n-p)!}{r!\,(n-p-r)!} \cos (n-p-2r)\,\omega_1 t \right] \times$$

$$\left[\sum_{s=0}^{p} \frac{p!}{s!\,(p-s)!} \cos (p-2s)\,\omega_2 t \right] \tag{26}$$

For this analysis, we are interested only in the terms A cos $\omega_2 t$ (to investigate cross modulation) and B cos $(2\omega_1 - \omega_2)t$ (third-order intermodulation). These terms can be obtained only as follows:

a. A cos $\omega_2 t$ ⟶ product of a constant and cos $\omega_2 t$

b. B cos $(2\omega_1 - \omega_2)t$ ⟶ from the product of cos $2\omega_1 t$ and cos $\omega_2 t$ via the relation

$$K \cos 2\omega_1 t \cos \omega_2 t = \frac{1}{2} K \cos (2\omega_1 - \omega_2)t + \frac{1}{2} K \cos (2\omega_1 + \omega_2)t$$

so that $B = \frac{1}{2} K$

Examination of the bracket expressions in equation 26 sets the following requirements:

For a.	$p - 2s = \pm 1$	p = odd	$s = \frac{p \mp 1}{2}$
	$n - p - 2r = 0$	$n - p = 0$ or even	$r = \frac{n-p}{2}$
	p = odd with $n - p = 0$ or even yields		n = odd
	as $p_{min} = 1$		$n_{min} = 1$
For b.	$p - 2s = \pm 1$	p = odd	$s = \frac{p \mp 1}{2}$
	$n - p - 2r = \pm 2$	$n - p$ = even	$r = \frac{n - p \mp 2}{2}$
	p = odd with $n - p$ = even yields		n = odd
	as $p_{min} = 1$		$n_{min} = 3$

From these requirements and equation 26, the amplitudes A and B can be deduced to be:

$$A = \sum_{n=1,3,5..}^{\infty} \alpha_n \sum_{p=1,3,5..}^{n} \frac{n!\, V_1^{n-p} V_2^{p}}{2^{n-1} \left[\left(\frac{n-p}{2}\right)!\right]^2 \left(\frac{p-1}{2}\right)! \left(\frac{p+1}{2}\right)!}$$

$$B = \sum_{n=3,5,7..}^{\infty} \alpha_n \sum_{p=1,3,5..}^{n} \frac{n!\, V_1^{n-p} V_2^{p}}{2^{n-1} \left(\frac{n-p}{2}-1\right)! \left(\frac{n-p}{2}+1\right)! \left(\frac{p-1}{2}\right)! \left(\frac{p+1}{2}\right)!}$$

By examinating, A, the ratio of the contribution of the factor (p + 2) and that of the factor p is:

$$\left(\frac{V_2}{V_1}\right)^2 \cdot \frac{(n-p)^2}{(p+1)(p+3)} \; n \geq 3$$

The same ratio with respect to B gives:

$$\left(\frac{V_2}{V_1}\right)^2 \cdot \frac{(n-p)^2 - 4}{(p+1)(p+2)} \; n > 3$$

These ratios are maximum for $p = p_{min} = 1$ for any given n. Assuming $\frac{V_1}{V_2} = 20$, even in the extreme case of a power series of 10 terms (n = 10), the total contribution for $p = 3, 5, 7 \ldots \infty$ is less than 3 percent of the contribution due to p = 1 alone for both A and B. As the practical measurements are normally taken for $\frac{V_1}{V_2} >> 20$, it is certainly justified to take only the contribution of p = 1, then:

$$A = \sum_{n=1,3,5..}^{\infty} \alpha_n \frac{n!\, V_1^{n-1} V_2}{2^{n-1} \left[\left(\frac{n-1}{2}\right)!\right]^2}$$

$$B = \sum_{n=3,5,7..}^{\infty} \alpha_n \frac{n!\, V_1^{n-1} V_2}{2^{n-1} \left(\frac{n-3}{2}\right)! \left(\frac{n+1}{2}\right)!}$$

The interesting part of the output amplitude can now be represented by:

$$V_{o_{int}} = \left[\sum_{n = 1,3,5..}^{\infty} \alpha_n V_1^{n-1} \frac{1}{2^{n-1}} \frac{n!}{\left[\left(\frac{n-1}{2}\right)!\right]^2} \right] V_2 \cos \omega_2 t + \left[\sum_{n = 3,5,7..}^{\infty} \alpha_n V_1^{n-1} \frac{1}{2^{n-1}} \frac{n!}{\left(\frac{n-3}{2}\right)! \left(\frac{n+1}{2}\right)!} \right] V_2 \cos (2\omega_1 - \omega_2)t \quad (27)$$

Equation 27 shows that the amplitude of cos $\omega_2 t$ is dependent on the amplitude V_1 of cos $\omega_1 t$.

Therefore, if $V_1 \cos \omega_1 t$ is modulated according to $\hat{V}_1 (1 + m \cos \omega_m t)$

where

m = modulation depth

ω_m = angular modulation frequency

Cross modulation will occur from ω_1 onto ω_2.

To quantitatively evaluate this cross modulation V_1^{n-1} in the first part of equation 27 has to be replaced by

$$\hat{V}_1^{n-1} (1 + m \cos \omega_m t)^{n-1}$$

If $m << 1$, the binomial series for $(1 + m \cos \omega_m t)^{n-1}$ can be truncated after two terms, or:

$$\hat{V}_1^{n-1} (1 + m \cos \omega_m t)^{n-1} \approx \hat{V}_1^{n-1} \left[1 + m (n-1) \cos \omega_m t\right]$$

The first part of equation 27 then becomes:

$$\left[\sum_{n = 1,3,5..}^{\infty} \alpha_n \hat{V}_1^{n-1} \frac{1}{2^{n-1}} \frac{n!}{\left[\left(\frac{n-1}{2}\right)!\right]^2} \left[1 + m (n-1) \cos \omega_m t\right] \right] V_2 \cos \omega_2 t$$

With $\alpha_n \hat{V}_1^{n-1} \cdot \frac{1}{2^{n-1}} \frac{n!}{\left[\left(\frac{n-1}{2}\right)!\right]^2} = X_n$, this can be rewritten as:

$$V_2 \sum_{n=1,3,5..}^{\infty} X_n \left[1 + m \frac{\sum_{n=1,3,5..}^{\infty} X_n (n-1)}{\sum_{n=1,3,5..}^{\infty} X_n} \cos \omega_m t \right] \cos \omega_2 t$$

This is of the form

$$C(1 + m_c \cos \omega_m t) \cos \omega_2 t$$

The cross-modulation depth m_c is then

$$m_c = \frac{\sum_{n=1,3,5..}^{\infty} X_n (n-1)}{\sum_{n=1,3,5..}^{\infty} X_n} m$$

For a small amount of cross modulation (practical case):

$$\sum_{n=1,3,5..}^{\infty} X_n \approx \alpha_1$$

and

$$\frac{m_c}{m} \approx \frac{1}{\alpha_1} \sum_{n=1,3,5..}^{\infty} X_n (n-1)$$

or

$$\frac{m_c}{m} \approx \frac{1}{\alpha_1} \sum_{n=1,3,5..}^{\infty} (n-1) \alpha_n V_1^{n-1} \frac{1}{2^{n-1}} \cdot \frac{n!}{\left[\left(\frac{n-1}{2}\right)!\right]^2}$$

As the first term vanishes (n - 1 = 0 for n = 1)

$$\frac{m_c}{m} \approx \frac{1}{\alpha_1} \sum_{n = 3,5,7..}^{\infty} (n-1)\, \alpha_n\, \hat{V}_1^{n-1}\, \frac{1}{2^{n-1}} \cdot \frac{n!}{\left(\frac{n-1}{2}\right)!\left(\frac{n-1}{2}\right)!}$$

Using the identities:

$$\left(\frac{n-1}{2}\right)! = \left(\frac{n-3}{2}\right)! \cdot \frac{n-1}{2}$$

and

$$\left(\frac{n-1}{2}\right)! = \left(\frac{n+1}{2}\right)! \cdot \frac{2}{n+1}$$

both valid simultaneously for $n \geqq 3$ yields

$$\frac{m_c}{m} \approx \frac{1}{\alpha_1} \sum_{n = 3,5,7..}^{\infty} (n+1)\, \alpha_n\, \hat{V}_1^{n-1}\, \frac{1}{2^{n-1}} \cdot \frac{n!}{\left(\frac{n-3}{2}\right)!\left(\frac{n+1}{2}\right)!} \tag{28}$$

The total cross-modulation factor $\frac{m_c}{m}$ is the sum of the individual cross-modulation factors $\frac{m_{c_n}}{m}$ $(n = 3,5,7\ldots)$ contributed by α_3, α_5, α_7, etc., respectively.

where

$$\frac{m_{c_n}}{m} = \frac{n+1}{\alpha_1}\, \alpha_n\, \hat{V}_1^{n-1}\, \frac{1}{2^{n-1}} \cdot \frac{n!}{\left(\frac{n-3}{2}\right)!\left(\frac{n+1}{2}\right)!} \tag{29}$$

The amplitude of the third-order intermodulation term for the unmodulated case

$$B = \sum_{n = 3,5,7..}^{\infty} \alpha_n\, V_1^{n-1}\, V_2\, \frac{1}{2^{n-1}} \cdot \frac{n!}{\left(\frac{n-3}{2}\right)!\left(\frac{n+1}{2}\right)!}$$

shows that $\frac{B}{V_2}$ can be regarded as the sum of the individual terms $\frac{B_n}{V_2}$ (n = 3, 5, 7..) contributed by the coefficients α_3, α_5, α_7.. etc., respectively, where

$$\frac{B_n}{V_2} = \alpha_n V_1^{n-1} \frac{1}{2^{n-1}} \frac{n!}{\left(\frac{n-3}{2}\right)! \left(\frac{n+1}{2}\right)!} \tag{30}$$

From equations 29 and 30 follows:

$$B_n = \frac{\alpha_1}{n+1} \frac{m_{c_n}}{m} V_2$$

or (31)

$$B = \frac{\alpha_1}{m} \sum_{n=3,5,7..}^{\infty} \frac{m_{c_n}}{n+1} V_2$$

In case the power series is truncated after three terms, equation 31 gives the familiar result

$$B = \frac{\alpha_1}{4} \cdot \frac{m_c}{m} V_2$$

which shows a fixed relation between the total cross-modulation factor $\frac{m_c}{m}$ and the total amount of third-order intermodulation B.

For n > 3, a fixed relation between the total cross modulation and the total amount of third-order intermodulation cannot be given without a specific knowledge of the factors α_1, α_3, α_5 .. etc., on account of the weighting factor $\frac{1}{n+1}$ in equation 31. By writing B and $\frac{m_c}{m}$ in the form

$$B = B_3 + B_5 + \ldots B_n = \frac{\alpha_1}{m} \left[\frac{m_{c_3}}{4} + - \frac{m_{c_5}}{6} \ldots + \frac{m_{c_n}}{n+1} \right]$$

and

$$\frac{m_c}{m} = \frac{1}{m} \left[m_{c_3} + m_{c_5} \ldots + m_{c_n} \right]$$

it can be seen that, taking into account positive and negative signs for α_n, and thus for m_{c_n}, a highly nonlinear region is theoretically conceivable, where it is possible that either one of the bracket parts of the expressions for B and m_c/m can become zero.

In this case, a situation would exist where intermodulation could be present without cross modulation or vice versa. This situation, however, should be highly critical and would be readily destroyed when changing bias conditions.

APPENDIX III

LIMITATIONS OF THE POWER SERIES METHOD

Assume a four-terminal network with a finite isolation between input and output. If any nonlinearity exists in this network, a signal frequency connected to the input will cause harmonic frequencies to appear at the output. These generated harmonics will feed back to the input and act as new input frequencies, generating more harmonics at the output which again are fed back to the input, etc., so that theoretically an infinite number of harmonics will be generated regardless of the inherent degree of nonlinearity.

Realization of this fact makes the validity of the power series representation $V_o = f(V_i)$ for this type of network very doubtful.

In this section, a concrete example will be given to show the failure of the power series method in the treatment of intermodulation and cross modulation of a network when a feedback is present between input and output.

Figure 16 represents a four-terminal network, N, terminated in a load resistance, R_L. Assume the following properties for N:

a. Infinite input impedance

b. Infinite output impedance

c. Infinite isolation between input and output

d. $V_o = f(V_i)$ is completely described by $V_o = \alpha V_i + \beta V_i^2$. Let Figure 17 represent a new four-terminal network, obtained from N, by adding some circuit elements. Let these circuit elements be chosen such that the following assumptions can be made

e. The impedance of the feedback circuit $|R_1 + \bar{Z}_2| >> R_L$

f. $|\bar{Z}_1| >> R_L$ for frequencies less than $\approx 3 \times$ signal frequency
$|\bar{Z}_1| = 0$ for frequencies $\approx 3 \times$ signal frequency and higher

g. $|\bar{Z}_2| = 0$ for frequencies of the order of $2 \times$ signal frequency
$|\bar{Z}_2| = \infty$ for all other frequencies

Because of stipulation g, for frequencies of the order of $2 \times$ signal frequency, a feedback from output to input will be present. Let the feedback factor be such that $\bar{k} V_o$ is coupled back to the input.

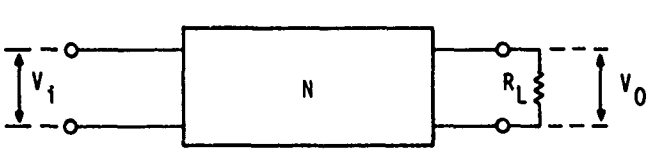

2-2268

Figure 16---Four-Terminal Network

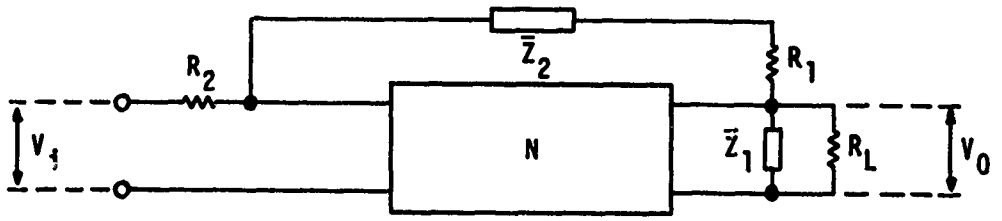

2-2269

Figure 17---Four-Terminal Network with Circuit Elements

With these assumptions and with $V_i = V_1 \cos \omega_1 t + V_2 \cos \omega_2 t$. The output spectrum can be examined on the specific frequency components of interest in the following manner. Assume

$$V_o = \bar{V}_{o_1} \cos \omega_1 t + \bar{V}_{o_2} \cos \omega_2 t + \bar{V}_{o_3} \cos 2\omega_1 t + \bar{V}_{o_4} \cos 2\omega_2 t + \bar{V}_{o_5} \cos (2\omega_1 - \omega_2)t + \bar{V}_{o_6} \cos (2\omega_2 - \omega_1)t \ldots + \ldots . \quad (32)$$

then

$$V_i^* = V_1 \cos \omega_1 t + V_2 \cos \omega_2 t + \bar{k}\ \bar{V}_{o_3} \cos 2\omega_1 t + \bar{k}\ \bar{V}_{o_4} \cos \omega_2 t \quad (33)$$

However:

$$V_o = \alpha V_1^* + \beta V_i^{*2} \quad (34)$$

Substitutions of equation 33 into 34, and considering only the terms of interest, gives:

$$V_o = (\alpha V_i + \beta \bar{k}\ V_1\ \bar{V}_{o_3}) \cos \omega_1 t + (\alpha V_2 + \beta \bar{k}\ V_2\ \bar{V}_{o_4}) \cos \omega_2 t + (\alpha \bar{k}\ \bar{V}_{o_3} + \tfrac{1}{2} \beta V_1^2) \cos 2\omega_1 t + (\alpha \bar{k}\ \bar{V}_{o_4} + \tfrac{1}{2} \beta V_2^2) \cos 2\omega_2 t + \beta \bar{k}\ V_1\ \bar{V}_{o_4} \cos (2\omega_2 - \omega_1)t + \beta \bar{k}\ V_2\ \bar{V}_{o_3} \cos (2\omega_1 - \omega_2)t \ldots$$

Equating these terms with the corresponding suggested terms of equation 32 yields:

a. $\overline{V}_{o_1} = \alpha V_1 + \beta \overline{k} V_1 \overline{V}_{o_3}$

b. $\overline{V}_{o_2} = \alpha V_2 + \beta \overline{k} V_2 \overline{V}_{o_4}$

c. $\overline{V}_{o_3} = \alpha \overline{k} \overline{V}_{o_3} + \frac{1}{2} \beta V_1^2$ or $\overline{V}_{o_3} = \frac{\beta V_1^2}{2 (1 - \alpha \overline{k})}$

d. $\overline{V}_{o_4} = \alpha \overline{k} \overline{V}_{o_4} + \frac{1}{2} \beta V_2^2$ or $\overline{V}_{o_4} = \frac{\beta V_2^2}{2 (1 - \alpha \overline{k})}$

e. $\overline{V}_{o_5} = \beta \overline{k} V_2 \overline{V}_{o_3}$

f. $\overline{V}_{o_6} = \beta \overline{k} V_1 \overline{V}_{o_4}$

Substituting the explicit expressions for V_{o_3} and V_{o_4} from c and d into a, b, e, and f gives:

$\left[\alpha V_1 + \frac{\overline{k} \beta^2 V_1^3}{2 (1 - \alpha \overline{k})} \right] \cos \omega_1 t$	fundamental component
$\left[\alpha V_2 + \frac{\overline{k} \beta^2 V_2^3}{2 (1 - \alpha \overline{k})} \right] \cos \omega_2 t$	fundamental component
$\left[\frac{\beta V_1^2}{2 (1 - \alpha \overline{k})} \right] \cos 2\omega_1 t$	second harmonic
$\left[\frac{\beta V_2^2}{2 (1 - \alpha \overline{k})} \right] \cos 2\omega_2 t$	second harmonic
$\left[\frac{\overline{k} \beta V_2 V_1^2}{2 (1 - \alpha \overline{k})} \right] \cos (2\omega_1 - \omega_2) t$	third-order intermodulation
$\left[\frac{\overline{k} \beta V_1 V_2^2}{2 (1 - \alpha \overline{k})} \right] \cos (2\omega_2 - \omega_1) t$	third-order intermodulation

As the amplitudes of $\cos \omega_1 t$ and $\cos \omega_2 t$ are only dependent on V_1 and V_2, respectively, no cross modulation can occur in the network of Figure 17. However, third-order intermodulation terms $\cos (2\omega_1 - \omega_2) t$ and $\cos (2\omega_2 - \omega_1) t$ are being generated.

The third-order intermodulation frequency $(2\omega_1 - \omega_2)$ in this case is generated by the second harmonic $2\omega_1$ which is fed back to the input where it mixes with ω_2 by way of the term βV_i^2 to create $2\omega_1 - \omega_2$ at the output.

As can be seen from the output components, the amplitude of the cos $(2\omega_1 - \omega_2)t$ term is proportional to the amplitude of $2\omega_1$, as could be expected.

A remarkable fact is that as far as the amplitude of the third-order intermodulation term is concerned, the functional relation of the power series treatment $C V_2 V_1^2 \cos (2\omega_1 - \omega_2)t$, where C is a constant, has been preserved.

As is shown in Appendix II, the general result, third-order intermodulation without cross modulation is incompatible with the power series method.

This is plausible because of the fact that by way of the power series these products can only arise when there is at least a cubic term $(j V_i^3)$ present. In the network of Figure 17, the highest inherent nonlinear term is quadratic (βV_i^2).

From the example given in this section, it can be concluded that a power series with constant coefficients cannot be used to analyze intermodulation, cross modulation, and similar frequency products, of a device when, for any integral part of this device, a feedback exists between input and output.

Unfortunately this rules out the majority of microwave devices, in particular, the distributed devices, which can be regarded as a chain of elementary networks, each corresponding to a specific volume element, so that generally a very tight coupling exists between input and output of each element.